NASA TECHNICAL NOTE

NASA TN D-2041

NASA TN D-2041

AN ANALYTICAL STUDY OF THE MAGNETIC FIELD ENCOUNTERED BY ARTIFICIAL EARTH SATELLITES IN CIRCULAR ORBITS

by Ward F. Hodge and W. Thomas Blackshear

Langley Research Center
Langley Station, Hampton, Va.

NATIONAL AERONAUTICS AND SPACE ADMINISTRATION • WASHINGTON, D. C. • FEBRUARY 1964

AN ANALYTICAL STUDY OF THE MAGNETIC FIELD ENCOUNTERED BY ARTIFICIAL EARTH SATELLITES IN CIRCULAR ORBITS

By Ward F. Hodge and W. Thomas Blackshear

Langley Research Center
Langley Station, Hampton, Va.

NATIONAL AERONAUTICS AND SPACE ADMINISTRATION

For sale by the Office of Technical Services, Department of Commerce,
Washington, D.C. 20230 -- Price $1.25

AN ANALYTICAL STUDY OF THE MAGNETIC FIELD ENCOUNTERED BY ARTIFICIAL EARTH SATELLITES IN CIRCULAR ORBITS

By Ward F. Hodge and W. Thomas Blackshear

SUMMARY

Analytical procedures for determining the magnetic field along the satellite orbit for any day in the year are developed on both an average and an instantaneous time basis. These methods are of interest in evaluating magnetic attitude-control schemes since the information they provide determines the magnitude and direction of the magnetic torque exerted on the satellite by the interaction of an onboard magnet with the earth's magnetic field.

The equations and methods presented are considered adequate for applications requiring attitude control within a few degrees. To illustrate typical results, plots of the average and instantaneous magnetic fields calculated from the equations given are presented for seven orbital inclinations ranging from 0° to 90° at orbital altitudes of 100, 300, and 500 nautical miles. These results show that the regression of the nodes of the satellite orbit has an effect that cannot be neglected.

INTRODUCTION

The achievement of artificial earth satellites has stimulated considerable interest in using the magnetic field of the earth for scientific purposes. Accordingly, the subject of satellite attitude control utilizing the interaction of onboard magnetic devices with the earth's magnetic field has continued to receive attention. The torque generated in this manner can be used to control the attitude of both oriented satellites and those which are spin stabilized.

For oriented satellites where any initial spin rate has been reduced to a negligible level, attitude control is possible by selective alinement of the satellite's magnetic axis with respect to the local direction of the earth's magnetic field. Several attitude-control systems based on this type of alinement are described in references 1 to 4. In the spin stabilized case, gyroscopic action will produce a change in attitude by causing the spin axis of the satellite to precess. (See refs. 5 and 6.) However, in either case, the attitude change for a given strength of the onboard magnet will be determined by the local intensity and direction of the earth's magnetic field along the orbital path. Analysis of magnetic attitude control therefore depends largely upon the magnitude and direction of the magnetic field experienced by the satellite in its orbit.

Another relevant consideration associated with magnetic attitude control concerns the variation of the satellite attitude with time. There are basically two cases to consider, the instantaneous attitude as a continuous function of time and the average attitude over some specified time interval. For a given application, the requirements of the control scheme being considered will determine which type of magnetic information is needed and the choice of coordinate system for describing the attitude motion. For these reasons, knowledge of both the instantaneous and the average magnetic field experienced by the satellite expressed in different coordinate systems is of interest.

Analytical procedures for determining both the instantaneous and the average magnetic field experienced by the satellite during any day in the year are developed and presented in this report. One procedure is a means of relating the time history of the instantaneous field over any day in the year with that for the first day. The other is a procedure for determining the average field for any day in the year. An analysis of the information obtained by these methods was made for test cases representing seven orbital inclinations at three orbital altitudes. The results of these calculations are presented on graphs in the report since this information should be useful in evaluating magnetic attitude-control schemes. To avoid involved calculations which must be properly referred to a specified epoch, only circular orbits subject to the assumptions noted in the text were considered.

The material contained in this report represents an extension of a study originally initiated to determine the feasibility of using a magnetic precession technique to maintain the attitude of a spinning satellite so the average daily direction of its spin axis remains toward the sun as the earth proceeds along its orbit about the sun. (See ref. 6.)

SYMBOLS

Rationalized mks units were generally used where applicable in the study. Exceptions occur where English and unrationalized mks units were used for convenience. Bars placed over symbols denote vectors whose magnitudes are indicated by omitting the bars. Symbols used to represent portions of equations are defined where they occur in the text and are not included in the following list of symbols.

a	equatorial radius of earth, meters
$\overline{B}$	magnetic field strength, webers/meter^2
$\hat{e}$	unit vector
$\overline{H}$	magnetic field intensity, amp/meter
h	altitude, meters or nautical miles
i	orbital inclination, deg

$\bar{L}$	torque, Newton-meter or pound-foot
$\bar{M}$	magnetic moment of earth, weber-meter
$\bar{r}$	position vector defining radius from center of earth to satellite, meters
r_A	mean radius of earth, meters
T	time interval, mean solar days
t	instantaneous time, min
V	potential of magnetic dipole, webers/meter
W	difference between longitude of satellite and longitude of ascending node, deg
X,Y,Z	ecliptic rectangular coordinates
x,y,z	geocentric rectangular coordinates
β	colatitude in geocentric polar coordinates, deg
Γ	angle between $\bar{B}$ and the Z-axis, radians
γ	angle between $\bar{B}$ and the ζ-axis, radians
θ	angular position of satellite in its orbital plane, deg
Λ	longitude in geocentric polar coordinates, deg
λ	longitude of ascending node of satellite orbit, deg
μ	angle between ζ- and z-axes, deg
μ_0	permeability of free space, webers/amp-meter
μ_r	relative permeability, dimensionless
ν	longitude in geomagnetic polar coordinates, deg
ξ,η,ζ	geomagnetic rectangular coordinates
Θ	colatitude in geomagnetic polar coordinates, deg
ϕ,α,ψ	Euler angles (see fig. 3), deg
$\dot{\phi}$	angular rate of earth about sun, radians/unit time
Ω	regression rate of nodes of satellite orbit, radians/unit time

ω axial rotation rate of earth, radians/unit time

ω_c circular velocity at orbital altitude, radians/unit time

Subscripts:

A average or mean value

I inertial

m,n indices for integers

0 initial value

r,Θ,ν quantities along geomagnetic polar coordinates

s satellite

X,Y,Z quantities along X,Y,Z coordinate axes

x,y,z quantities along x,y,z coordinate axes

ξ,η,ζ quantities along ξ,η,ζ coordinate axes

PROCEDURE

The equations describing the analytical procedures used in the study are developed in this section of the report. In order to derive such equations, it is first necessary to choose a suitable mathematical description of the earth's magnetic field. The spherical harmonic representation outlined in appendix A is generally considered the most accurate one available. However, the equations developed herein were based on the dipole field obtained when only the first three terms of the spherical harmonic representation are retained. (See appendix A.) This approximation gives sufficient accuracy for the purposes of the study.

The development of these procedures was essentially accomplished in two steps. First, the expressions for the instantaneous field were obtained by establishing a correspondence between the satellite's position and the dipole field. Then by making a suitable choice of variables, these equations were integrated in closed form to obtain the expressions for the average field. Both sets of equations are given in two coordinate systems of interest for purposes of magnetic attitude control.

Assumptions

In addition to assuming a dipole representation for the earth's magnetic field, the study was based on the following general assumptions:

(1) The satellite remains at constant altitude in circular orbit about the earth.

(2) The orbit of the earth about the sun is also treated as circular.

(3) All perturbations except the regression of the nodes of the satellite orbit are considered negligible in comparison with the inaccuracy introduced by dipole representation of the earth's magnetic field.

It should be mentioned that these assumptions are made without regard to satellite geometry and may not be very suitable for configurations which are noticeably influenced by effects such as those due to gravity gradient and solar radiation pressure. At the altitudes considered, the most significant of the perturbations which are neglected in making these assumptions is aerodynamic drag which may be ignored since it only tends to make the orbit more circular.

Correlation of Satellite Position With Magnetic Field Along Its Orbit

To specify the magnetic field encountered by a satellite, it is necessary to establish a correspondence between its position and the field intensity vector along the orbital path. Defining a Cartesian coordinate system and a set of spherical polar coordinates as shown in figure 1, the satellite position in a circular orbit can be specified as a function of time for a given choice of r and i by the following relations:

$$\theta = \omega_c t + \theta_0$$

$$\lambda = kt + \lambda_0$$

where

$$k = -(\omega + \Omega)$$

in which

$$\Omega = 10 \cos i \left(\frac{a}{r}\right)^{7/2}$$

gives the regression of the nodes of the satellite orbit in degrees per day for orbits of low eccentricity. (See ref. 7.)

Geomagnetic coordinates.- The dipole representing the earth's magnetic field is fixed with respect to the earth and for this reason it is convenient to consider the satellite's position in coordinates rotating with the earth. This choice permits the x- and ξ-axes to be taken coincident along the line of intersection of the geomagnetic and geocentric equatorial planes which is located about 21° east of Greenwich as indicated in figure 2.

The rectangular components of the position vector $\bar{r}$ in the two coordinate systems are:

$$\bar{r} = \hat{e}_\xi(r \sin \Theta \cos \nu) + \hat{e}_\eta(r \sin \Theta \sin \nu) + \hat{e}_\zeta(r \cos \Theta)$$

and

$$\bar{r} = \hat{e}_x(r \sin \beta \cos \Lambda) + \hat{e}_y(r \sin \beta \sin \Lambda) + \hat{e}_z(r \cos \beta)$$

where the corresponding relations between the unit vectors

$$\hat{e}_\xi = \hat{e}_x$$

$$\hat{e}_\eta = \hat{e}_y \cos \mu + \hat{e}_z \sin \mu$$

$$\hat{e}_\zeta = -\hat{e}_y \sin \mu + \hat{e}_z \cos \mu$$

are obtained from figure 2 by means of trigonometry. Therefore, the position vector $\bar{r}$ in the two coordinate systems is related by the following matrix equation:

$$\begin{Bmatrix} \sin \Theta \cos \nu \\ \sin \Theta \sin \nu \\ \cos \Theta \end{Bmatrix} = \begin{pmatrix} 1 & 0 & 0 \\ 0 & \cos \mu & \sin \mu \\ 0 & -\sin \mu & \cos \mu \end{pmatrix} \begin{Bmatrix} \sin \beta \cos \Lambda \\ \sin \beta \sin \Lambda \\ \cos \beta \end{Bmatrix}$$

By using this equation, trigonometric identities, and the following relationships obtained from figure 1,

$$\Lambda = \lambda + W$$

$$\tan W = \tan \theta \cos i$$

$$\cos \beta = \sin \theta \sin i$$

$$\sin \beta = \frac{\cos \theta}{\cos W}$$

the geomagnetic components of the earth's dipole field given in appendix A (eqs. (A3)) can be expressed in the following form:

$$\left.\begin{aligned} \bar{B}_\xi &= -\frac{3M}{2r^3}\left(a \cos \mu \sin i - \frac{1}{2} b \sin \mu\right) \\ \bar{B}_\eta &= -\frac{3M}{2r^3}\left(c \cos 2\mu \sin i + \frac{1}{4} d \sin 2\mu\right) \\ \bar{B}_\zeta &= \frac{3M}{2r^3}\left(c \sin 2\mu \sin i + \frac{1}{2} d \sin^2 \mu + \frac{1}{3} e\right) \end{aligned}\right\} \quad (1)$$

where

$$a = C \cos \lambda - D \sin \lambda$$

$$b = E \sin 2\lambda + F \cos 2\lambda$$

$$c = C \sin \lambda + D \cos \lambda$$

$$d = E \cos 2\lambda - F \sin 2\lambda - e$$

$$e = 2 - 3 \sin^2 i(1 - \cos 2\theta)$$

in which

$$C = \sin 2\theta$$

$$D = \cos i(1 - \cos 2\theta)$$

$$E = \sin^2 i + (1 + \cos^2 i)\cos 2\theta$$

$$F = 2C \cos i$$

Thus, equations (1) give the geomagnetic rectangular components of the magnetic field experienced by the satellite as functions of its position with respect to the rotating earth. The components of the magnetic field in x,y,z coordinates differ from those given by equations (1) only by a rotation through the constant angle μ (as indicated in eqs. (B1)). For this reason, the overall characteristics of the field will be the same for both coordinate systems and only the geomagnetic equations are discussed.

Ecliptic coordinates.- For applications where it is necessary to account for the earth's motion about the sun, it is advantageous to determine the field intensity vector in terms of rotating ecliptic coordinates. The ecliptic components of $\bar{B}$ as indicated in figure 3 can be obtained conveniently by means of the Euler angle transformation given in appendix B. The resulting equations (eqs. (B2b)) can be expressed in the following form by substituting equations (1) and using trigonometric identities:

$$\left.\begin{aligned}
\bar{B}_X &= -\frac{3M}{2r^3}\left[\cos \mu \sin i(P \cos \phi - Q \sin \phi \cos \alpha) - \frac{1}{2} \sin \mu(R \cos \phi + S \sin \phi \cos \alpha) - K_X\right] \\
\bar{B}_Y &= -\frac{3M}{2r^3}\left[\cos \mu \sin i(P \sin \phi + Q \cos \phi \cos \alpha) - \frac{1}{2} \sin \mu(R \sin \phi - S \cos \phi \cos \alpha) - K_Y\right] \\
\bar{B}_Z &= -\frac{3M}{2r^3}\left[\sin \alpha(P \cos \mu \sin i + \frac{1}{2} Q \sin \mu) - K_Z\right]
\end{aligned}\right\} \qquad (2)$$

where

$$P = C \cos(\lambda + \psi) - D \sin(\lambda + \psi)$$

$$Q = C \sin(\lambda + \psi) + D \cos(\lambda + \psi)$$

$$R = E \sin(2\lambda + \psi) + F \cos(2\lambda + \psi)$$

$$S = E \cos(2\lambda + \psi) - F \sin(2\lambda + \psi)$$

$$K_X = \frac{1}{6} e\left(a_{12} \sin \mu + 2a_{13} \cos \mu\right) + a_{13}(c \sin \mu \sin i)$$

$$K_Y = \frac{1}{6} e\left(a_{22} \sin \mu + 2a_{23} \cos \mu\right) + a_{23}(c \sin \mu \sin i)$$

$$K_Z = \frac{1}{6} e\left(a_{32} \sin \mu + 2a_{33} \cos \mu\right) + a_{33}(c \sin \mu \sin i)$$

in which the $a_{m,n}$ are elements of the Euler angle transformation matrix given in appendix B. Equations (2) give the components of $\overline{B}$ experienced by the satellite as functions of its position in an ecliptic coordinate system that rotates about the Z-axis once a year relative to the sun.

Method for Obtaining the Average Magnetic Field

The instantaneous time histories of $\overline{B}$ along the orbital path of the satellite in the geomagnetic and ecliptic coordinate systems are given by equations (1) and (2). These expressions are functions of time and may be integrated in the following manner to obtain the average magnetic field experienced by the satellite during a given interval of time:

$$\overline{B}_A = \frac{1}{T} \int_0^T \hat{e}_m B(t) dt$$

where the $\hat{e}_m B(t)$ represents the vector components of $\overline{B}$.

Geomagnetic coordinates.- Since all the time-dependent angles involved in equations (1) and (2) except ϕ complete at least one cycle in a period nearly equal to that of the earth's axial rotation, it is convenient to choose a time period of one mean solar day as the integration interval. Integrating equations (1) on this basis gives the following expressions for the average geomagnetic components of the field over 1 day:

$$\left.\begin{aligned}
\bar{B}_{\xi A} &= -\frac{3M}{2Tr^3}\left(a_A \cos\mu \sin i - \frac{1}{2} b_A \sin\mu\right) \\
\bar{B}_{\eta A} &= -\frac{3M}{2Tr^3}\left(c_A \cos 2\mu \sin i + \frac{1}{4} d_A \sin 2\mu\right) \\
\bar{B}_{\zeta A} &= \frac{3M}{2Tr^3}\left(c_A \sin 2\mu \sin i + \frac{1}{2} d_A \sin^2\mu + \frac{1}{3} e_A\right)
\end{aligned}\right\} \qquad (3)$$

where

$$a_A = -\frac{1}{2}\left\{\frac{1+\cos i}{2\omega_c + k}\left[\cos(G - A) - \cos(\lambda_0 + A_0)\right]\right.$$

$$\left. + \frac{1-\cos i}{2\omega_c - k}\left[\cos(G + A) - \cos(\lambda_0 - A_0)\right] - \frac{2\cos i}{k}\left(\cos G - \cos\lambda_0\right)\right\}$$

$$b_A = -\frac{1}{2}\left\{\frac{(1+\cos i)^2}{2(\omega_c + k)}\left[\cos(2G - A) - \cos(2\lambda_0 + A_0)\right]\right.$$

$$\left. - \frac{(1-\cos i)^2}{2(\omega_c - k)}\left[\cos(2G + A) - \cos(2\lambda_0 - A_0)\right] + \frac{\sin^2 i}{k}\left(\cos 2G - \cos 2\lambda_0\right)\right\}$$

$$c_A = \frac{1}{2}\left\{\frac{1+\cos i}{2\omega_c + k}\left[\sin(G - A) + \sin(\lambda_0 + A_0)\right]\right.$$

$$\left. + \frac{1-\cos i}{2\omega_c - k}\left[\sin(G + A) + \sin(\lambda_0 - A_0)\right] - \frac{2\cos i}{k}\left(\sin G + \sin\lambda_0\right)\right\}$$

$$d_A = -\frac{1}{2}\left\{\frac{(1+\cos i)^2}{2(\omega_c + k)}\left[\sin(2G - A) + \sin(2\lambda_0 + A_0)\right]\right.$$

$$\left. - \frac{(1-\cos i)^2}{2(\omega_c - k)}\left[\sin(2G + A) + \sin(2\lambda_0 - A_0)\right] + \frac{\sin^2 i}{k}\left(\sin 2G + \sin 2\lambda_0\right) + 2e_A\right\}$$

$$e_A = \left[\left(2 - 3\sin^2 i\right) + \frac{3\sin^2 i}{2\omega_c}\left(\sin A - \sin A_0\right)\right]$$

in which

$$G = \Omega T - \lambda_0$$

$$A = 2\omega_c T + A_0$$

$$A_0 = 2\theta_0$$

Ecliptic coordinates.- The transformation to ecliptic coordinates introduces additional time-dependent quantities since two of the three Euler angles are given by:

$$\psi = \omega t + \psi_0$$

$$\phi = \dot{\phi} t + \phi_0$$

This situation poses no difficulty and equations (2) can be integrated in closed form in the same manner as equations (1) by redefining two of the time-dependent angles in the following form:

$$\lambda' = \lambda + \psi = k't + \lambda_0'$$

and

$$\lambda'' = 2\lambda + \psi = k''t + \lambda_0''$$

where

$$k' = -\Omega$$

$$k'' = -(2\Omega + \omega)$$

and

$$\lambda_0' = \lambda_0 + \psi_0$$

$$\lambda_0'' = 2\lambda_0 + \psi_0$$

This step reduces the number of time-dependent angles involved in integrating any portion of equations (2) to a maximum of three. However, the order can be reduced from three to two by holding ϕ constant which changes by less than 1^o during the 1-day integration interval. Comparisons with results obtained when the variation of ϕ is included in the integration shows that no noticeable error is incurred by treating ϕ as a constant. The integration of equations (2) with ϕ constant yields the following expressions for the 1-day averages of the ecliptic components of the field:

$$\left.\begin{aligned}
\bar{B}_{XA} &= -\frac{3M}{2Tr^3}\left[\cos\mu\sin i\left(P_A\cos\phi - Q_A\sin\phi\cos\alpha\right)\right.\\
&\qquad\left. -\frac{1}{2}\sin\mu\left(R_A\cos\phi + S_A\sin\phi\cos\alpha\right) - K_{XA}\right]\\
\bar{B}_{YA} &= -\frac{3M}{2Tr^3}\left[\cos\mu\sin i\left(P_A\sin\phi + Q_A\cos\phi\cos\alpha\right)\right.\\
&\qquad\left. -\frac{1}{2}\sin\mu\left(R_A\sin\phi - S_A\cos\phi\cos\alpha\right) - K_{YA}\right]\\
\bar{B}_{ZA} &= -\frac{3M}{2Tr^3}\left[\sin\alpha\left(P_A\cos\mu\sin i + \frac{1}{2}Q_A\sin\mu\right) - K_{ZA}\right]
\end{aligned}\right\} \qquad (4)$$

where

$$P_A = -\frac{1}{2}\left\{\frac{(1+\cos i)\left[\cos(G-A) - \cos(\lambda_0 + A_0)\right]}{2\omega_c - \Omega}\right.$$

$$\left. + \frac{(1-\cos i)\left[\cos(G+A) - \cos(\lambda_0 - A_0)\right]}{2\omega_c + \Omega} + \frac{2\cos i(\cos G - \cos\lambda_0)}{\Omega}\right\}$$

$$Q_A = \frac{1}{2}\left\{\frac{(1+\cos i)\left[\sin(G-A) + \sin(\lambda_0 + A_0)\right]}{2\omega_c - \Omega}\right.$$

$$\left. + \frac{(1-\cos i)\left[\sin(G+A) + \sin(\lambda_0 - A_0)\right]}{2\omega_c + \Omega} + \frac{2\cos i(\sin G + \sin\lambda_0)}{\Omega}\right\}$$

$$R_A = -\frac{1}{2}\left\{\frac{(1+\cos i)^2\left[\cos(2G-A) - \cos(2\lambda_0 + A_0)\right]}{2\omega_c - 2\Omega - \omega}\right.$$

$$\left. - \frac{(1-\cos i)^2\left[\cos(2G+A) - \cos(2\lambda_0 - A_0)\right]}{2\omega_c + 2\Omega + \omega} - \frac{2\sin^2 i(\cos 2G - \cos 2\lambda_0)}{2\Omega + \omega}\right\}$$

$$S_A = -\frac{1}{2}\left\{\frac{(1 + \cos i)^2\left[\sin(2G - A) + \sin(2\lambda_0 + A_0)\right]}{2\omega_c - 2\Omega - \omega}\right.$$

$$\left. - \frac{(1 - \cos i)^2\left[\sin(2G + A) + \sin(2\lambda_0 - A_0)\right]}{2\omega_c + 2\Omega + \omega} - \frac{2\sin^2 i(\sin 2G + \sin 2\lambda_0)}{2\Omega + \omega}\right\}$$

$$K_{XA} = \frac{1}{3} e_A \cos\mu \sin\alpha \sin\phi + \frac{1}{4}\sin\mu \sin^2 i\left(K_1 \cos\phi - K_2 \cos\alpha \sin\phi\right)$$

$$+ \left(c_A \sin\mu \sin i\right)\sin\alpha \sin\phi$$

$$K_{YA} = \frac{1}{3} e_A \cos\mu \sin\alpha \cos\phi + \frac{1}{4}\sin\mu \sin^2 i\left(K_1 \sin\phi + K_2 \cos i \cos\phi\right)$$

$$- \left(c_A \sin\mu \sin i\right)\sin\alpha \cos\phi$$

$$K_{ZA} = \frac{1}{3} e_A \cos\mu \cos\alpha + \frac{1}{4}\sin\mu \sin^2 i\left(K_2 \sin\alpha\right) + \left(c_A \sin\mu \sin i\right)\cos\alpha$$

$$K_1 = \left(\cos A - \cos A_0\right)\left(\frac{1}{2\omega_c + \omega} - \frac{1}{2\omega_c - \omega}\right)$$

$$K_2 = \left(\sin A - \sin A_0\right)\left(\frac{1}{2\omega_c + \omega} + \frac{1}{2\omega_c - \omega}\right)$$

Note that the third terms in P_A and Q_A vanish when Ω is zero.

Reduced form of equations.- Reasonably good results can be obtained by deleting the angle A and its initial value A_0 from equations (3) and (4). When this approximation is made, these equations reduce to

$$\bar{B}_{\xi A} = \frac{3M}{2Tr^3}\left[C_1 \cos\mu \sin i\left(\cos G - \cos\lambda_0\right) - \frac{1}{2} C_2 \sin\mu\left(\cos 2G - \cos 2\lambda_0\right)\right]\Bigg\} \quad (3a)$$

(Equations continued on next page)

$$\left.\begin{aligned}
\bar{B}_{\eta A} &= -\frac{3M}{2Tr^3}\left\{C_1 \cos 2\mu \sin i\left(\sin G + \sin \lambda_0\right)\right. \\
&\qquad \left. - \frac{1}{4}\sin 2\mu\left[C_2\left(\sin 2G + \sin 2\lambda_0\right) + \left(2 - 3\sin^2 i\right)T\right]\right\} \\
\bar{B}_{\zeta A} &= \frac{3M}{2Tr^3}\left\{C_1 \sin 2\mu \sin i\left(\sin G + \sin \lambda_0\right) - \frac{1}{2}\sin^2\mu\left[C_2\left(\sin 2G + \sin 2\lambda_0\right)\right.\right. \\
&\qquad \left.\left. + \left(2 - 3\sin^2 i\right)T\right] + \frac{1}{3}\left(2 - 3\sin^2 i\right)T\right\}
\end{aligned}\right\} \tag{3a}$$

and

$$\left.\begin{aligned}
\bar{B}_{XA} &= \frac{3M}{2Tr^3}\left[W_1 \cos \phi + \left(W_2 \cos \alpha + W_3 \sin \alpha\right)\sin \phi\right] \\
\bar{B}_{YA} &= \frac{3M}{2Tr^3}\left[W_1 \sin \phi - \left(W_2 \cos \alpha + W_3 \sin \alpha\right)\cos \phi\right] \\
\bar{B}_{ZA} &= -\frac{3M}{2Tr^3}\left(W_2 \sin \alpha - W_3 \cos \alpha\right)
\end{aligned}\right\} \tag{4a}$$

where

$$W_1 = C_3 \cos \mu \sin i\left(\cos G - \cos \lambda_0\right) + C_4\left(\cos 2G - \cos 2\lambda_0\right)$$

$$W_2 = C_3 \cos \mu \sin i\left(\sin G + \sin \lambda_0\right) + C_4\left(\sin 2G + \sin 2\lambda_0\right)$$

$$W_3 = C_1 \sin \mu \sin i\left(\sin G + \sin \lambda_0\right) + \frac{1}{3}\left(2 - 3\sin^2 i\right)T \cos \mu$$

in which

$$C_1 = \frac{1}{2}\left(\frac{1 + \cos i}{2\omega_c + k} + \frac{1 - \cos i}{2\omega_c - k} - \frac{2 \cos i}{k}\right)$$

$$C_2 = \frac{1}{2}\left[\frac{\left(1 + \cos i\right)^2}{2\left(\omega_c + k\right)} - \frac{\left(1 - \cos i\right)^2}{2\left(\omega_c - k\right)} + \frac{\sin^2 i}{k}\right]$$

$$C_3 = \frac{1}{2}\left(\frac{1 + \cos i}{2\omega_c - \Omega} + \frac{1 - \cos i}{2\omega_c + \Omega} + \frac{2 \cos i}{\Omega}\right)$$

$$C_4 = \frac{1}{4}\left[\frac{(1 - \cos i)^2}{2(\omega_c + \Omega) + \omega} - \frac{(1 + \cos i)^2}{2(\omega_c - \Omega) - \omega} + \frac{2 \sin^2 i}{2\Omega + \omega}\right]$$

Note that the third term in C_3 vanishes when Ω is zero. Equations (3a) and (4a) shorten the calculations considerably and give results that are within a few percent of those given by the original equations. The results given by equations (3) and (3a) always agreed within 4 percent, and those given by equations (4) and (4a) within 1 percent for the cases considered in this study.

ANALYSIS

An analysis of the average and instantaneous magnetic fields given by equations (1) to (4) is made for test cases covering satellite lifetimes up to 2 years. These cases were calculated for seven orbital inclinations ranging from 0° to 90° at orbital altitudes of 100, 300, and 500 nautical miles. The use of equations (1) to (4) in devising analytical procedures for obtaining the average and instantaneous magnetic fields encountered by the satellite any day in the year is described in detail. To facilitate the discussion, the results for the geomagnetic and ecliptic coordinate systems are treated separately. Finally, this information is discussed in terms of torque to indicate its use for attitude-control purposes.

Geomagnetic System

The magnitude of the instantaneous field intensity vector in these coordinates is

$$B = \sqrt{B_\xi{}^2 + B_\eta{}^2 + B_\zeta{}^2}$$

and the angle it makes with the ζ-axis (see fig. 2) is

$$\gamma = \tan^{-1} \frac{\sqrt{B_\xi{}^2 + B_\eta{}^2}}{B_\zeta}$$

This information is presented in figure 4 for all seven orbital inclinations at each of the three altitudes. These curves represent the instantaneous time histories of $\bar{B}$ and γ for the first day of the satellite lifetime which is assumed to start with the initial values of θ and λ set to zero. All the curves exhibit a sinusoid due to the satellite crossing the geomagnetic equator twice per orbit superimposed upon one due to the daily rotation of the dipole field about the earth's axis of rotation as would be expected.

Comparisons of the results for different days in the year indicate that the time histories of $\overline{B}$ and γ for any day are contained in the corresponding ones for the first day, and that the curves for the two days differ mainly by their starting times which are determined by θ_0 and λ_0. By locating the time on the curve for γ plotted against t for a given day when λ corresponds to λ_0 for the first day, then moving from this point to the nearest time when θ is zero it was found that the two curves always coincide within the accuracy of the plots. Identical results were obtained for the corresponding $\overline{B}$ curves. Since λ changes by a small amount during the time involved, the error due to moving away from the correct location of λ to bring θ into phase is negligible and could not be detected in the results.

To illustrate this procedure, a portion of the time histories of γ for the first day and a test day beginning 100 days later are plotted in figure 5 for an orbital inclination of 30° at an altitude of 300 nautical miles. The figure shows the initial portion of the curve for γ plotted against t for the first day and the region of the curve for the test day where λ corresponds to λ_0 for the first day. The point where this occurs is located about 280 minutes after the beginning of the test day as indicated in figure 5(b). By moving along the curve a distance Δt from λ to the nearest time when θ is zero which occurs about 306 minutes after the test day begins, it can be seen that the region of the curve starting at this point coincides with the initial portion of the curve for the first day.

Thus, the time histories of $\overline{B}$ and γ presented for one day in figure 4 can be used for any day in the year. These results indicate that Ω, which causes λ_0 to be different from zero at the start of any given day, continuously displaces the time histories of $\overline{B}$ and γ in time at a rate equal to that of the regression of the nodes of the satellite orbit.

In a similar fashion, the average magnetic field experienced by the satellite may be specified in terms of its magnitude and direction which are given by:

$$B_A = \sqrt{B_{\xi A}^2 + B_{\eta A}^2 + B_{\zeta A}^2}$$

and

$$\gamma_A = \tan^{-1} \frac{\sqrt{B_{\xi A}^2 + B_{\eta A}^2}}{B_{\zeta A}}$$

where γ_A is the angle between $\overline{B}_A$ and the ζ-axis as shown in figure 6.

The calculations made indicate that B_A and γ_A oscillate with small changes in amplitude at a frequency equal to the regression rate of the nodes of the satellite orbit. For the three altitudes considered, B_A and γ_A and their variations in amplitude change with the inclination of the satellite orbit. Since

both quantities are essentially sinusoids, their mean values for each inclination may be plotted as in figure 7 to illustrate generally the variation of B_A and γ_A with i.

These curves show that B_A decreases to zero in the vicinity of 55° and then increases to half its maximum value at 90° for each of the three altitudes. The corresponding curves for γ_A indicate that $\overline{B}_A$ reverses direction at an inclination near 55° such that it then points below instead of above the geomagnetic equator. The region between 45° and 60° is shown dashed on the plot since more data than were calculated would be needed to define this portion of the curve. Only one curve for γ_A is presented since the overall geometric shape of the dipole field does not change enough over the range of the three altitudes used to produce any appreciable variation in the three curves.

Within the accuracy to which B_A and γ_A were calculated, their amplitude variations are too small to plot except for orbital inclinations near 55° where the combined effect of both oscillations is maximum. This behavior is of minor importance since B_A is much too small in this region to be effective in changing the attitude of the satellite. Thus, the average field intensity vector encountered by the satellite is essentilly fixed in magnitude and direction with respect to rotating geomagnetic coordinates. When viewed in inertial coordinates, $\overline{B}_A$ would therefore appear to rotate once a day relative to the ζ_I-axis in a nearly circular path having its center on the z_I-axis as shown in figure 6.

Ecliptic System

The instantaneous time histories of $\overline{B}$ in ecliptic coordinates were not used in this study and no results are presented for this case. For applications where the instantaneous time histories of $\overline{B}$ in ecliptic coordinates are of interest, equations (2) can be used to obtain the desired information. The simple procedure devised for relating the time histories of $\overline{B}$ at different days in the year breaks down in the ecliptic system because three instead of two initial angles must be correlated in time. Although it might be possible to extend the procedure to handle this case, it appears the resulting process would be too cumbersome to be very useful.

By following the approach used in the preceding section, the corresponding expressions for the average magnitude and direction of the field intensity vector in rotating ecliptic coordinates are

$$B_A = \sqrt{B_{XA}^2 + B_{YA}^2 + B_{ZA}^2}$$

and

$$\Gamma_A = \tan^{-1} \frac{\sqrt{B_{XA}^2 + B_{YA}^2}}{B_{ZA}}$$

where Γ_A is the angle between $\bar{B}_A$ and the Z-axis as shown in figure 8.

The calculations of these quantities show that B_A is also essentially constant when determined in ecliptic coordinates. Therefore, the variation of B_A with i may be plotted in the same manner as was done for the geomagnetic system. This information is presented in figure 9 which shows that B_A decreases with i from its maximum at 0^o to half this value at 90^o. A comparison of figures 7 and 9 show that B_A has the same values in both coordinate systems for equatorial and polar orbits, but differs considerably for all inclinations between 0^o and 90^o because the time dependency to be integrated is not the same in both coordinate systems except for these two special cases where the effect of the difference in time dependency vanishes.

The angular position of $\bar{B}_A$ in ecliptic coordinates does not exhibit the nearly constant behavior with respect to time it has when defined in geomagnetic coordinates. The plots of Γ_A against ϕ presented in figure 10 indicate Γ_A oscillates with a period equal to $2\pi/\Omega$. Thus, Γ_A oscillates with the same frequency as γ_A, but with much larger variations in amplitude.

Figure 10 shows that $\bar{B}_A$ also reverses direction at orbital inclinations near 55^o when expressed in ecliptic coordinates. Curves for the 0^o and 90^o inclinations are not presented in figure 10 since Ω, and hence the oscillation, vanishes in each case. The values of Γ_A for these cases are essentially constant at all three altitudes and have the same approximate values of 0.409 and 2.732 radians for inclinations of 0^o and 90^o, respectively. These values of Γ_A are equal to α and $\alpha + \pi$; thus, $\bar{B}_A$ is oriented parallel to the earth's spin axis and points along the positive z-axis for the 0^o inclination and in the negative direction for the 90^o case.

In addition to the larger amplitude variations, $\bar{B}_A$ rotates relative to rotating ecliptic coordinates. Plots of the resultant of $\bar{B}_{XA}$ and $\bar{B}_{YA}$ (not presented) show that this quantity, which is the numerator in the expression for Γ_A, rotates once a year in the X,Y plane since ϕ determines its angular position as shown in figure 8. Referring to the sketch in figure 8, it is evident that $\bar{B}_A$ makes one revolution per year about the Z-axis while oscillating back and forth in the plane passing through the Z-axis perpendicular to the line of nodes of the earth's orbit about the sun. These results indicate that the plane containing $\bar{B}_A$ has a fixed orientation in inertial space since the X,Y,Z coordinate system which rotates at the rate $\dot{\phi}$ completes one revolution a year. For the special cases where Ω is zero (i = 0^o or 90^o), Γ_A is constant and $\bar{B}_A$ has

a fixed orientation parallel to the earth's spin axis as discussed in the preceding paragraph.

Attitude Control

As indicated in the introduction, the interaction of the magnetic field of the earth with that of an onboard magnet will produce a resultant torque on the satellite that can be used to control its attitude. This torque is given by:

$$\bar{L}_A = \bar{M}_S \times \bar{B}_A$$

where $\bar{M}_S$ is the magnetic moment vector of the onboard magnet. Although presented in terms of the average field, the following discussion of attitude control applies to the instantaneous field as well.

For nonspinning satellites, $\bar{L}_A$ will act so as to aline $\bar{M}_S$ with $\bar{B}_A$. The resulting motion is to a first approximation that of a damped simple harmonic oscillator which is discussed at length in reference 2. Essentially what happens is that $\bar{M}_S$ will track $\bar{B}_A$ reasonably well after the oscillatory motion damps out. The relative strength of $\bar{L}_A$ is the dominant factor which determines the duration of the oscillatory motion and how closely the satellite will track the local direction of $\bar{B}_A$ along its orbital path. Tracking accuracies of the order of 2° or less for the Transit and INJUN satellites are indicated in reference 2.

The magnetic torque will cause the spin axis to precess like a gyroscope in the case of spinning satellites. If the magnetic moment vector of the onboard magnet is alined with the spin axis, $\bar{L}_A$ will cause $\bar{M}_S$ to precess in a conical path about $\bar{B}_A$ as indicated in figure 11. As the spin axis precesses, $\bar{L}_A$ will describe a plane perpendicular to $\bar{B}_A$ in accordance with the cross-product relationship between the three vectors. It is evident that the manner in which $\bar{B}_A$ moves relative to the coordinate system will be exhibited in the precessional motion of the spin axis. Thus, it can be seen that the magnitude and direction of the magnetic field along the satellite orbit determines the magnetic attitude-control possibilities for both oriented and spin-stabilized satellites.

A passive magnetic precession technique to maintain the average daily attitude of the spin axis toward the sun as the earth proceeds along its orbit about the sun was considered for the 150-foot space station described in reference 6. By referring to figure 11, which also illustrates the situation for this application, the desired motion is to precess the spin axis in the X,Y plane at the rate $\dot{\phi}$ such that the angle between $\bar{M}_S$ and the X-axis remains as small as possible. It is evident from figure 11 that the optimum path of $\bar{M}_S$ lies in the plane containing $\bar{L}_A$. If the angle between $\bar{M}_S$ and $\bar{B}_A$ is 90°, $\bar{M}_S$ will precess in a sinusoidal path of amplitude Γ_A with respect to the X,Y plane. Thus, $\bar{M}_S$ cannot be held any closer to the X,Y plane than $\pm\Gamma_A$. The minimum value of Γ_A occurs when the orbital inclination is zero; thus, an equatorial orbit represents the optimum case. Unfortunately, the minimum value of Γ_A is equal to α

(about 23.45°) and is too large to satisfy the requirements of this particular application.

In regard to the onboard magnet, either permanent or electromagnets can be used. The power and weight requirements for electromagnets may be calculated by the method used in reference 1. For permanent magnets, the magnet weight required to produce a given value of M_S can be calculated by using the procedure given in reference 4. Their calculations indicate that currently available magnet materials will provide about 0.001 pound-foot of torque per pound of magnet at an altitude of 300 nautical miles.

CONCLUSIONS

The results of an analytical study of the magnetic field along circular orbits indicate the following conclusions:

1. The regression of the nodes of the satellite orbit has a noticeable effect on both the average and instantaneous magnetic fields experienced by a satellite in circular orbit which cannot be neglected.

2. The regression of the nodes causes the time histories of the instantaneous magnetic field vector for any 2 days in the year to differ by a displacement in time that includes smaller effects due to other differences in the initial conditions for each day.

3. The average magnetic field vector, determined on a daily basis by integration in closed form, is nearly constant in magnitude and direction relative to rotating geocentric coordinates; and in ecliptic coordinates the average field vector oscillates with constant magnitude at the same rate as the regression of the nodes in a plane fixed in inertial space.

Langley Research Center,
National Aeronautics and Space Administration,
Langley Station, Hampton, Va., August 30, 1963.

APPENDIX A

THE EARTH'S MAGNETIC FIELD

Spherical Harmonic Representation

The magnetic field of the earth may be considered representable as a conservative field of force in which a force vector referred to as the field intensity $\overline{H}$ exists at every point in the field. Since the current densities present on or near the earth are extremely small, its magnetic field may also be assumed to be irrotational. Under these conditions the field may be specified by a scalar potential function V that satisfies Laplace's equation

$$\nabla^2 V = 0$$

where the field intensity is given by the gradient of V

$$\overline{H} = -\nabla V$$

If the field due to external sources is neglected, the general solution to Laplace's equation for a spherical boundary at $r = a$ reduces to

$$V = a \sum_{n=1}^{\infty} \sum_{m=0}^{n} P_n^m \cos \beta \left(\frac{a}{r}\right)^{n+1} \left(g_n^m \cos m\Lambda + h_n^m \sin m\Lambda\right)$$

where the $P_n^m \cos \beta$ are multiples of associated Legendre functions and the g_n^m and h_n^m are the experimentally determined Gaussian coefficients. (See ref. 8.)

Dipole Representation

For applications where less accuracy is needed, a reasonably good approximation of the earth's magnetic field can be obtained by retaining only the first three of the Gaussian coefficients. When this approximation is made, the preceding spherical harmonic expansion of the earth's magnetic field gives the potential due to the first coefficient g_1^0 as

$$V_1^0 = g_1^0 \frac{a^3}{r^2} \cos \beta$$

which is exactly the potential of a simple dipole located at the center of the earth with its magnetic moment vector

$$M_1^0 = g_1^0 a^3$$

directed along the earth's axis of rotation. Similarly, the second and third coefficients g_1^1 and h_1^1 correspond to simple dipoles which are perpendicular to each other and lie at the center of the earth in the plane of the equator. The geographic orientation of the three orthogonal dipoles and their resultant $\bar{H}$ is illustrated in figure 12. The resultant field obtained in this manner is frequently used in dipole representations of the earth's magnetic field and is the same as that of a single dipole whose potential is given by

$$V = H \frac{a^3}{r^2} \cos \mu$$

where

$$H = \sqrt{\left(g_1^0\right)^2 + \left(g_1^1\right)^2 + \left(h_1^1\right)^2}$$

This resultant dipole is also located at the center of the earth as would be expected, but is inclined at a fixed angle μ to the axis of rotation as shown in figure 12. It should be noted that the geomagnetic polar axis, defined as the line containing $\bar{H}$, does not coincide with the familiar terrestrial magnetic poles which are also indicated on the drawing in figure 12. The magnetic moment vector of the resultant dipole in unrationalized mks units is given by

$$\bar{M} = \bar{H}a^3$$

which also lies along the geomagnetic polar axis. Depending upon which determinations of the Gaussian coefficients and the earth's equatorial radius are used, the magnitudes of $\bar{M}$ and μ will vary slightly. The values used in this study are given in table I and correspond to those contained in reference 9.

TABLE I.- PHYSICAL CONSTANTS

Quantity	Symbol	Value
Permeability of free space	μ_0	$4\pi \times 10^{-7}$ weber/amp-meter
Magnetic moment of earth*	M	8.1×10^{15} weber-meter
Mean radius of earth	r_A	6.3712213×10^6 meters
Equatorial radius of earth	a	6.3783880×10^6 meters
Inclination of earth's spin axis to ecliptic polar axis	α	23.45°
Angle between ζ- and z-axis	μ	11.50°
Axial rotation rate of earth	ω	2π radians/day
Average angular rate of earth about sun	$\dot{\phi}$	$\frac{2\pi}{365.25}$ radians/day

*This value of M is given in unrationalized mks units and must be divided by μ_0 to convert it to rationalized mks units.

The remaining step in representing the earth's magnetic field by a dipole is to define suitable coordinates for specifying $\bar{H}$ or its components at any point in the field. By choosing the geomagnetic polar axis as the prime reference, a rectangular geomagnetic coordinate system may be defined as shown in figure 2. In this system, the ζ-axis is along the prime reference axis with the ξ- and η-axes taken to form an orthogonal system. It is convenient to obtain the components of $\bar{H}$ in terms of geomagnetic spherical polar coordinates which are also defined in figure 2, and then transform the results to the desired coordinate system by means of rotation matrices. (See appendix B.)

The potential of the resultant dipole expressed in vector form is

$$V = \frac{\bar{M} \cdot \bar{r}}{r^3}$$

In polar form, the potential becomes

$$V = -\frac{M}{r^2} \cos \Theta \tag{A1}$$

where the minus sign arises because of the manner in which Θ is defined. (See fig. 2.)

By using the relation

$$\bar{B} = \mu_r \mu_0 \bar{H}$$

in which the relative permeability μ_r may be taken as unity for air, the field strength can be expressed as

$$\bar{B} = -\nabla V$$

where the unrationalized value of M given in table I is used in equation (A1) to eliminate the permeability of free space μ_0 from both sides of the equation.

Taking the gradient of V

$$\bar{B} = -\nabla V$$

$$\bar{B} = \hat{e}_r\left(\frac{-\partial V}{\partial r}\right) + \frac{\hat{e}_\Theta}{r}\left(\frac{-\partial V}{\partial \Theta}\right) + \frac{\hat{e}_\nu}{r \sin \Theta}\left(\frac{-\partial V}{\partial \nu}\right)$$

$$\bar{B} = \hat{e}_r B_r + \hat{e}_\Theta B_\Theta + \hat{e}_\nu B_\nu$$

gives the polar components of the field as

$$\left.\begin{aligned} \bar{B}_r &= -\hat{e}_r \frac{2M \cos \Theta}{r^3} \\ \bar{B}_\Theta &= -\hat{e}_\Theta \frac{M \sin \Theta}{r^3} \\ \bar{B}_\nu &= 0 \end{aligned}\right\} \qquad \text{(A2)}$$

from which the components of $\bar{B}$ along the ξ, η, ζ axes are:

$$\bar{B}_\xi = \left(\bar{B}_r \sin \Theta + \bar{B}_\Theta \cos \Theta\right) \cos \nu$$

$$\bar{B}_\eta = \left(\bar{B}_r \sin \Theta + \bar{B}_\Theta \cos \Theta\right) \sin \nu$$

$$\bar{B}_\zeta = \bar{B}_r \cos \Theta - \bar{B}_\Theta \sin \Theta$$

Upon substituting equations (A2) in these expressions, the rectangular geomagnetic components of $\bar{B}$ become

$$\left.\begin{aligned} \bar{B}_\xi &= -\frac{3M}{r^3} \cos \Theta \sin \Theta \cos \nu \\ \bar{B}_\eta &= -\frac{3M}{r^3} \cos \Theta \sin \Theta \sin \nu \\ \bar{B}_\zeta &= \frac{M}{r^3}\left(1 - 3 \cos^2 \Theta\right) \end{aligned}\right\} \qquad \text{(A3)}$$

APPENDIX B

COORDINATE TRANSFORMATIONS

Rotating Coordinates

Equations (1) correlate the satellite position with the geomagnetic rectangular components of $\overline{B}$ given by equations (A3) in terms of rotating coordinates fixed in the earth. Since the ξ,η,ζ and x,y,z coordinate systems differ only by a rotation through the angle μ as shown in figure 2, the geocentric rectangular components of $\overline{B}$ in rotating coordinates may be obtained from equations (1) by means of the matrix relationship:

$$\begin{Bmatrix} \overline{B}_x \\ \overline{B}_y \\ \overline{B}_z \end{Bmatrix} = \begin{pmatrix} 1 & 0 & 0 \\ 0 & \cos\mu & -\sin\mu \\ 0 & \sin\mu & \cos\mu \end{pmatrix} \begin{Bmatrix} \overline{B}_\xi \\ \overline{B}_\eta \\ \overline{B}_\zeta \end{Bmatrix} \tag{B1}$$

To obtain the rotating ecliptic components of $\overline{B}$, it is easiest to employ Euler angles such as those defined in figure 3. The product of the matrices corresponding to successive rotations through the three Euler angles ϕ,α,ψ is the matrix (denoted by $\underset{\sim}{A}$)

$$\underset{\sim}{A} = \begin{pmatrix} a_{11} & a_{12} & a_{13} \\ a_{21} & a_{22} & a_{23} \\ a_{31} & a_{32} & a_{33} \end{pmatrix}$$

whose elements are

$$a_{11} = \cos\psi\cos\phi - \cos\alpha\sin\phi\sin\psi$$

$$a_{12} = -(\sin\psi\cos\phi + \cos\alpha\sin\phi\cos\psi)$$

$$a_{13} = \sin\alpha\sin\phi$$

$$a_{21} = \cos\psi\sin\phi + \cos\alpha\cos\phi\sin\psi$$

$$a_{22} = -(\sin\psi\sin\phi - \cos\alpha\cos\phi\cos\psi)$$

$$a_{23} = -\sin\alpha\cos\phi$$

$$a_{31} = \sin \alpha \sin \psi$$

$$a_{32} = \sin \alpha \cos \psi$$

$$a_{33} = \cos \alpha$$

In matrix notation the desired transformation is:

$$\begin{Bmatrix} \overline{B}_X \\ \overline{B}_Y \\ \overline{B}_Z \end{Bmatrix} = \underset{\sim}{A} \begin{Bmatrix} \overline{B}_x \\ \overline{B}_y \\ \overline{B}_z \end{Bmatrix} \tag{B2a}$$

which may be written in scalar equation form as:

$$\left.\begin{aligned} \overline{B}_X &= a_{11}\overline{B}_\xi + a_{12}\left(\overline{B}_\eta \cos \mu - \overline{B}_\zeta \sin \mu\right) + a_{13}\left(\overline{B}_\eta \sin \mu + \overline{B}_\zeta \cos \mu\right) \\ \overline{B}_Y &= a_{21}\overline{B}_\xi + a_{22}\left(\overline{B}_\eta \cos \mu - \overline{B}_\zeta \sin \mu\right) + a_{23}\left(\overline{B}_\eta \sin \mu + \overline{B}_\zeta \cos \mu\right) \\ \overline{B}_Z &= a_{31}\overline{B}_\xi + a_{32}\left(\overline{B}_\eta \cos \mu - \overline{B}_\zeta \sin \mu\right) + a_{33}\left(\overline{B}_\eta \sin \mu + \overline{B}_\zeta \cos \mu\right) \end{aligned}\right\} \tag{B2b}$$

Inertial Coordinates

Simple rotation matrices can also be used to obtain the magnetic field encountered by the satellite in inertial coordinates. Since the ξ,η,ζ and x,y,z coordinate systems are fixed with respect to each other, the transformation of either system to a corresponding inertial system involves only the angular motion due to the earth's rotation. The displacement ψ of the x-axis from some fixed reference such as the autumnal equinox is illustrated in figure 6. Therefore, the geomagnetic and geocentric inertial components of $\overline{B}$ are:

$$\begin{Bmatrix} \overline{B}_{\xi I} \\ \overline{B}_{\eta I} \\ B_{\zeta I} \end{Bmatrix} = \begin{pmatrix} \cos \psi & -\sin \psi & 0 \\ \sin \psi & \cos \psi & 0 \\ 0 & 0 & 1 \end{pmatrix} \begin{Bmatrix} \overline{B}_\xi \\ \overline{B}_\eta \\ \overline{B}_\zeta \end{Bmatrix} \tag{B3}$$

and

$$\begin{Bmatrix} \bar{B}_{xI} \\ \bar{B}_{yI} \\ \bar{B}_{zI} \end{Bmatrix} = \begin{pmatrix} \cos\psi & -\sin\psi & 0 \\ \sin\psi & \cos\psi & 0 \\ 0 & 0 & 1 \end{pmatrix} \begin{Bmatrix} \bar{B}_{x} \\ \bar{B}_{y} \\ \bar{B}_{z} \end{Bmatrix} \tag{B4}$$

The inertial ecliptic components of $\bar{B}$ may be obtained in a similar fashion by rotating the X,Y,Z coordinate system through the angle ϕ to account for the motion of the earth about the sun. (See fig. 8.) The resulting transformation gives:

$$\begin{Bmatrix} \bar{B}_{XI} \\ \bar{B}_{YI} \\ \bar{B}_{ZI} \end{Bmatrix} = \begin{pmatrix} \cos\phi & \sin\phi & 0 \\ -\sin\phi & \cos\phi & 0 \\ 0 & 0 & 1 \end{pmatrix} \begin{Bmatrix} \bar{B}_{X} \\ \bar{B}_{Y} \\ \bar{B}_{Z} \end{Bmatrix} \tag{B5}$$

REFERENCES

1. White, John S., Shigemoto, Fred H., and Bourquin, Kent: Satellite Attitude Control Utilizing the Earth's Magnetic Field. NASA TN D-1068, 1961.

2. Fischell, Robert E.: Passive Magnetic Attitude Control for Earth Satellites. Preprint 62-8, American Astronautical Soc., Jan. 1962.

3. Lomax, J. B., Brandstatter, J. J., Ablow, C. M., and Nelson, R. A.: A Study of the Magnetic Stabilization of a Passive Satellite. RADC TR-61-105 (Contract AF 30(602)-2245), Stanford Res. Inst. (Menlo Park, Calif.), Apr. 1961.

4. Adams, James J., and Brissenden, Roy F.: Satellite Attitude Control Using a Combination of Inertia Wheels and a Bar Magnet. NASA TN D-626, 1960.

5. Bandeen, W. R., and Manger, W. P.: Angular Motion of the Spin Axis of the Tiros I Meteorological Satellite Due to Magnetic and Gravitational Torques. NASA TN D-571, 1961.

6. Langley Research Center Staff: A Report on the Research and Technological Problems of Manned Rotating Spacecraft. NASA TN D-1504, 1962.

7. King-Hele, D. G., and Merson, R. H.: Satellite Orbits in Theory and Practice. Jour. British Interplanetary Soc., vol. 16, no. 8, July-Aug. 1958, pp. 446-471.

8. Fougere, Paul: The Terrestrial Magnetic Field. Space and Planetary Environments, Shea L. Valley, ed., Air Force Surveys in Geophysics No. 139 (AFCRL-62-270), Air Force Cambridge Res. Labs., Jan. 1962, pp. 15-31.

9. Vinti, John P.: Theory of the Spin of a Conducting Satellite in the Magnetic Field of the Earth. Rep. No. 1020, Ballistic Res. Labs., Aberdeen Proving Ground, July 1957.

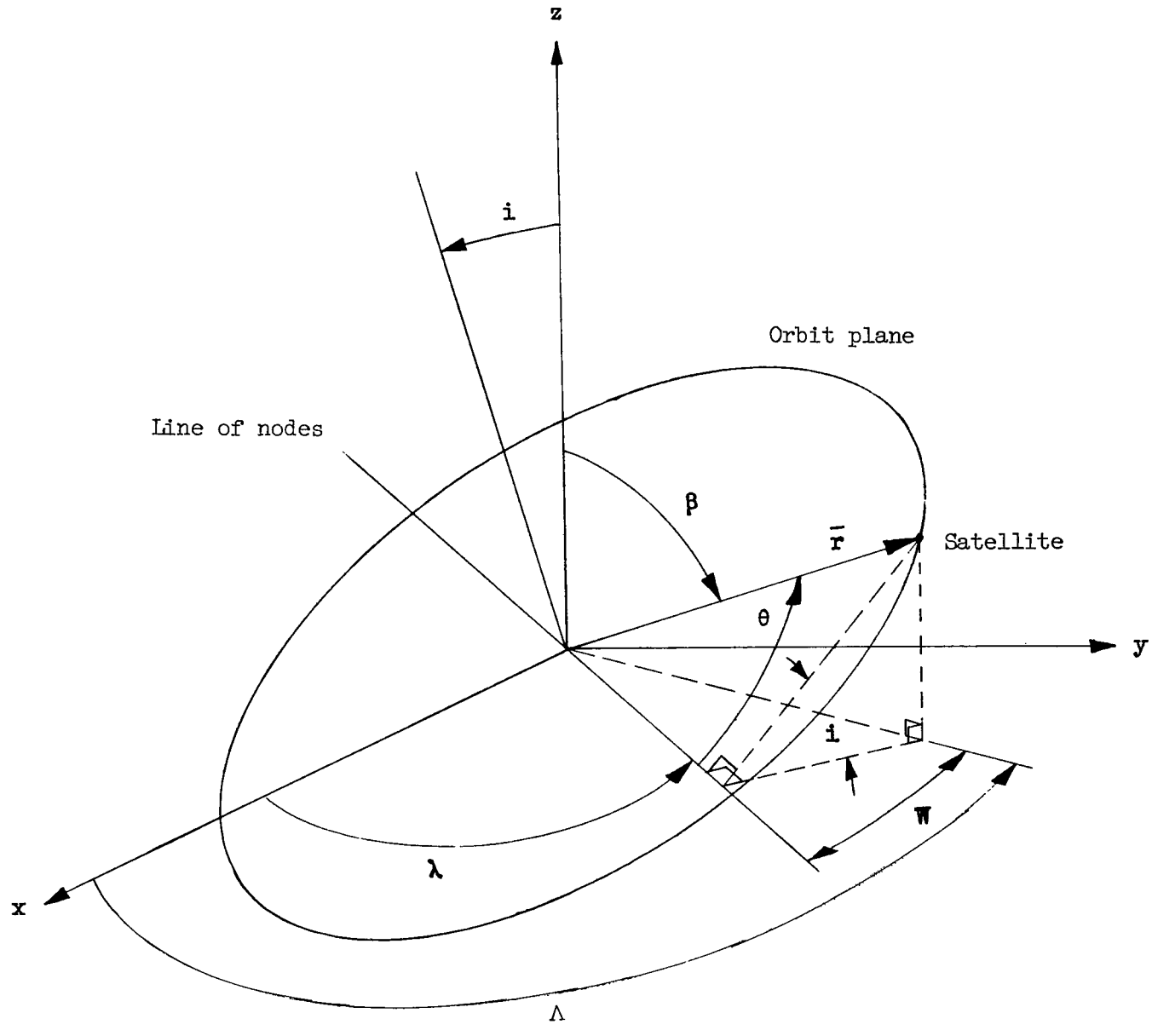

Figure 1.- Geocentric position coordinates.

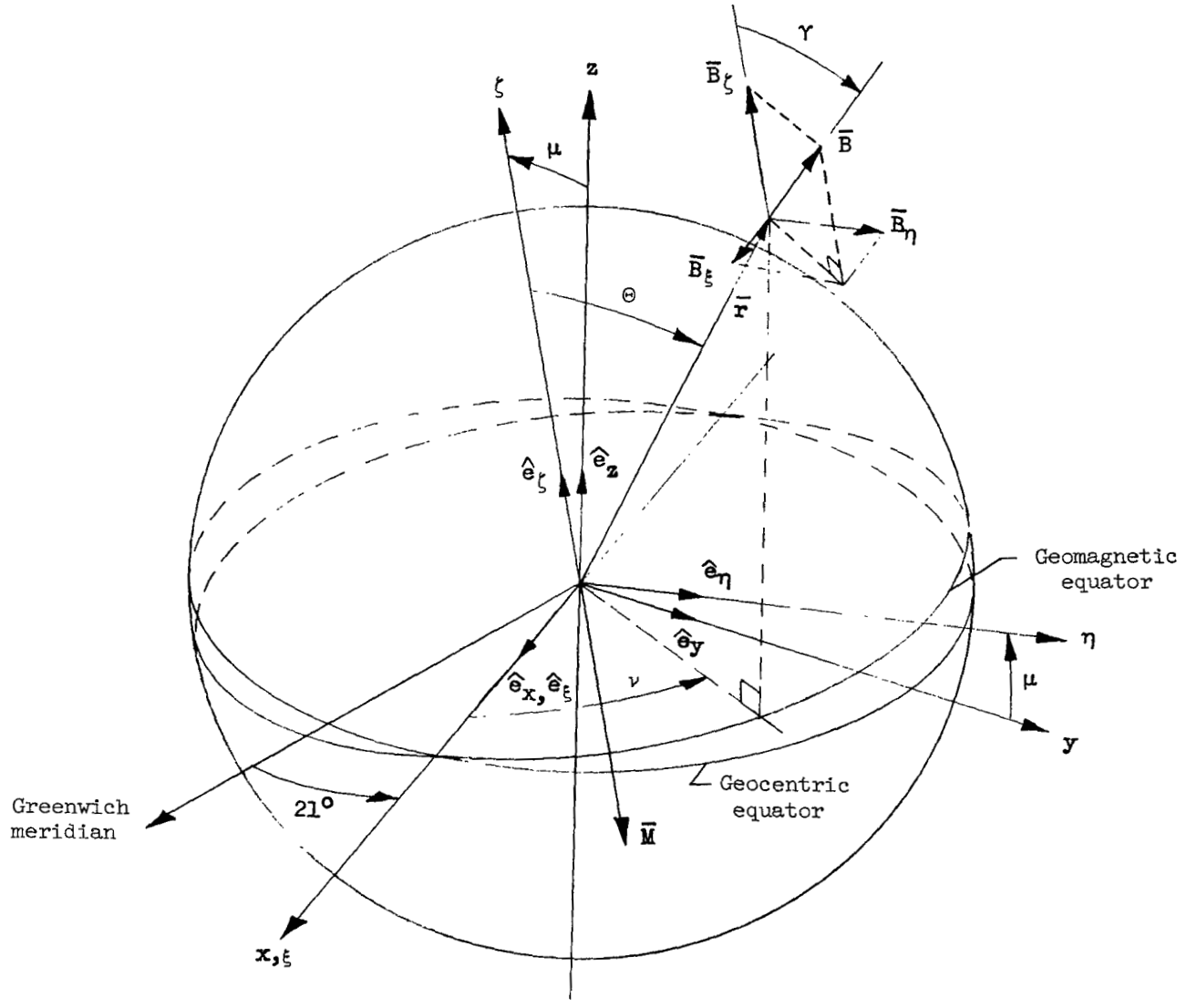

Figure 2.- Orientation of geomagnetic and geocentric coordinate systems.

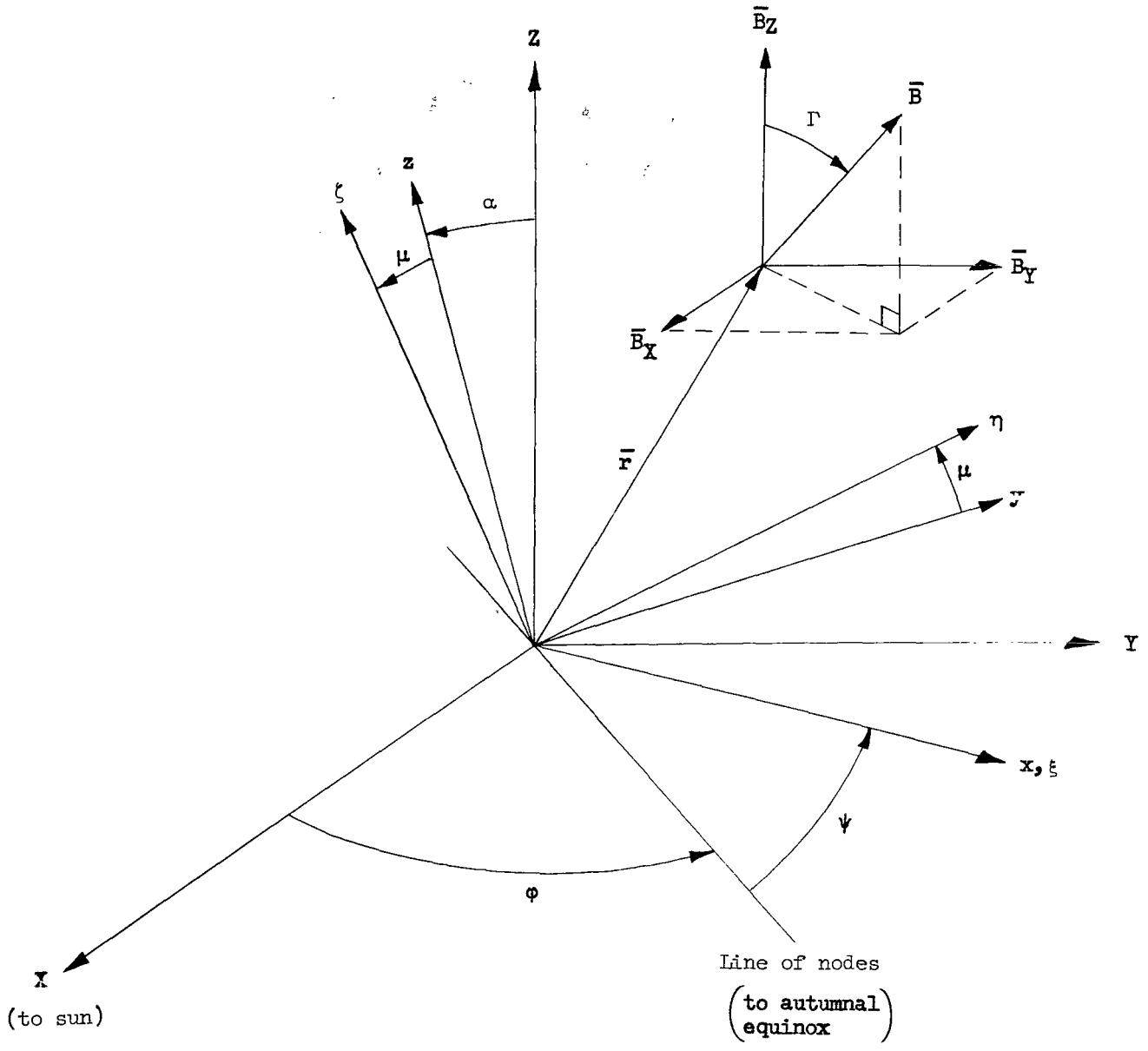

Figure 3.- Rotating ecliptic coordinate system and Euler angles.

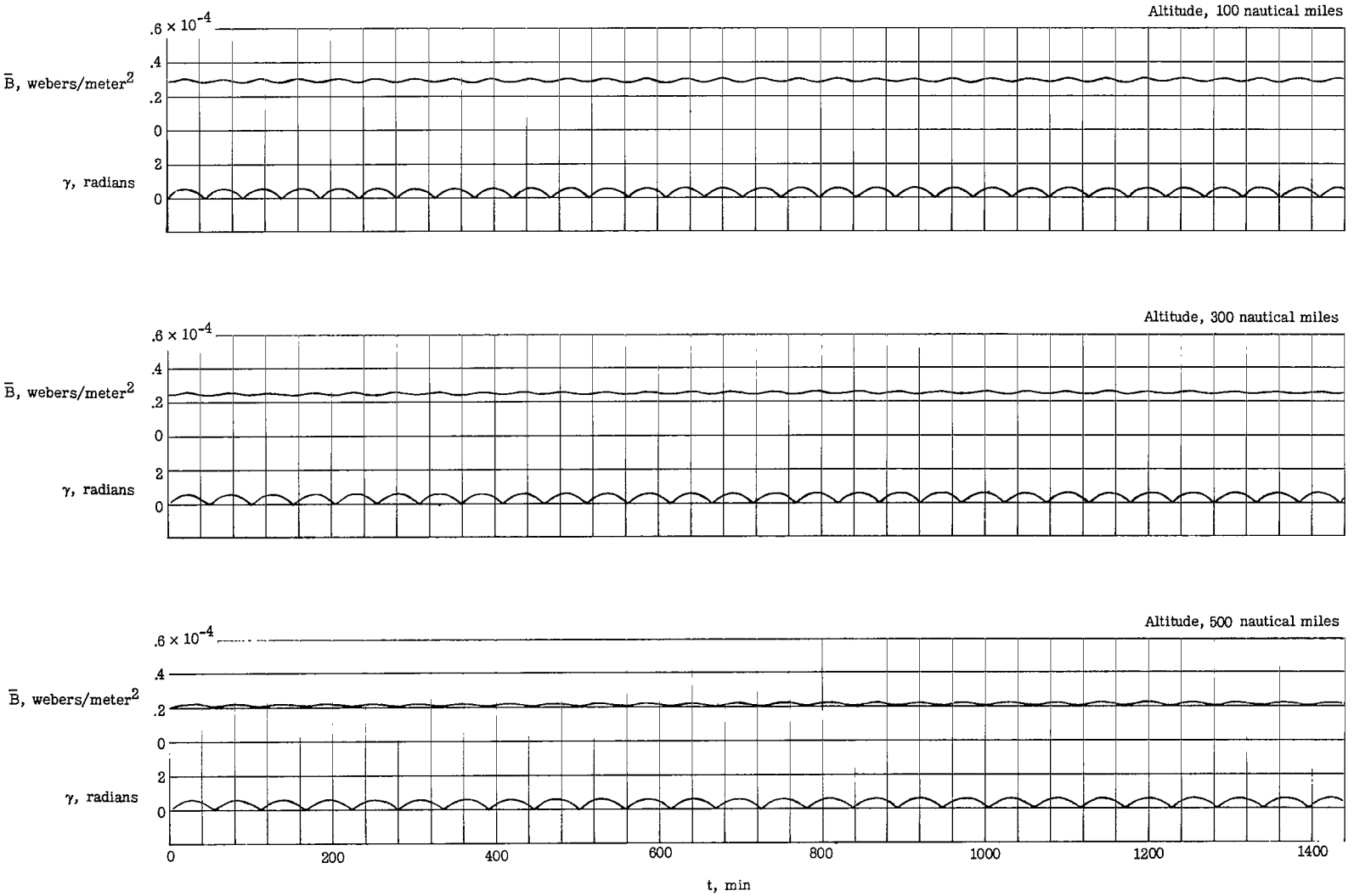

(a) $i = 0^{\circ}$.

Figure 4.- Time histories of the geomagnetic instantaneous field along the satellite orbit for 1 day.

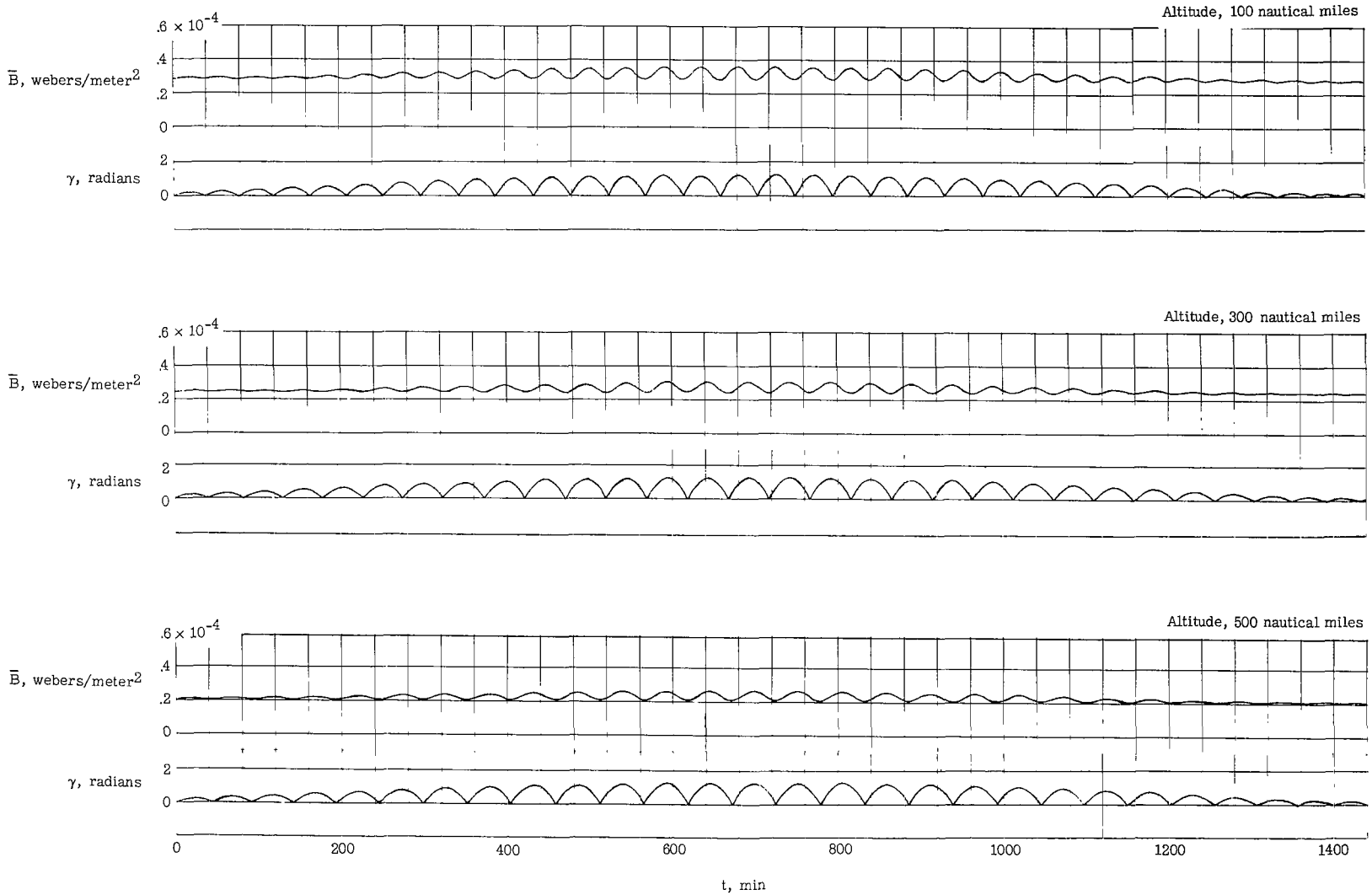

(b) i = 15°.

Figure 4.- Continued.

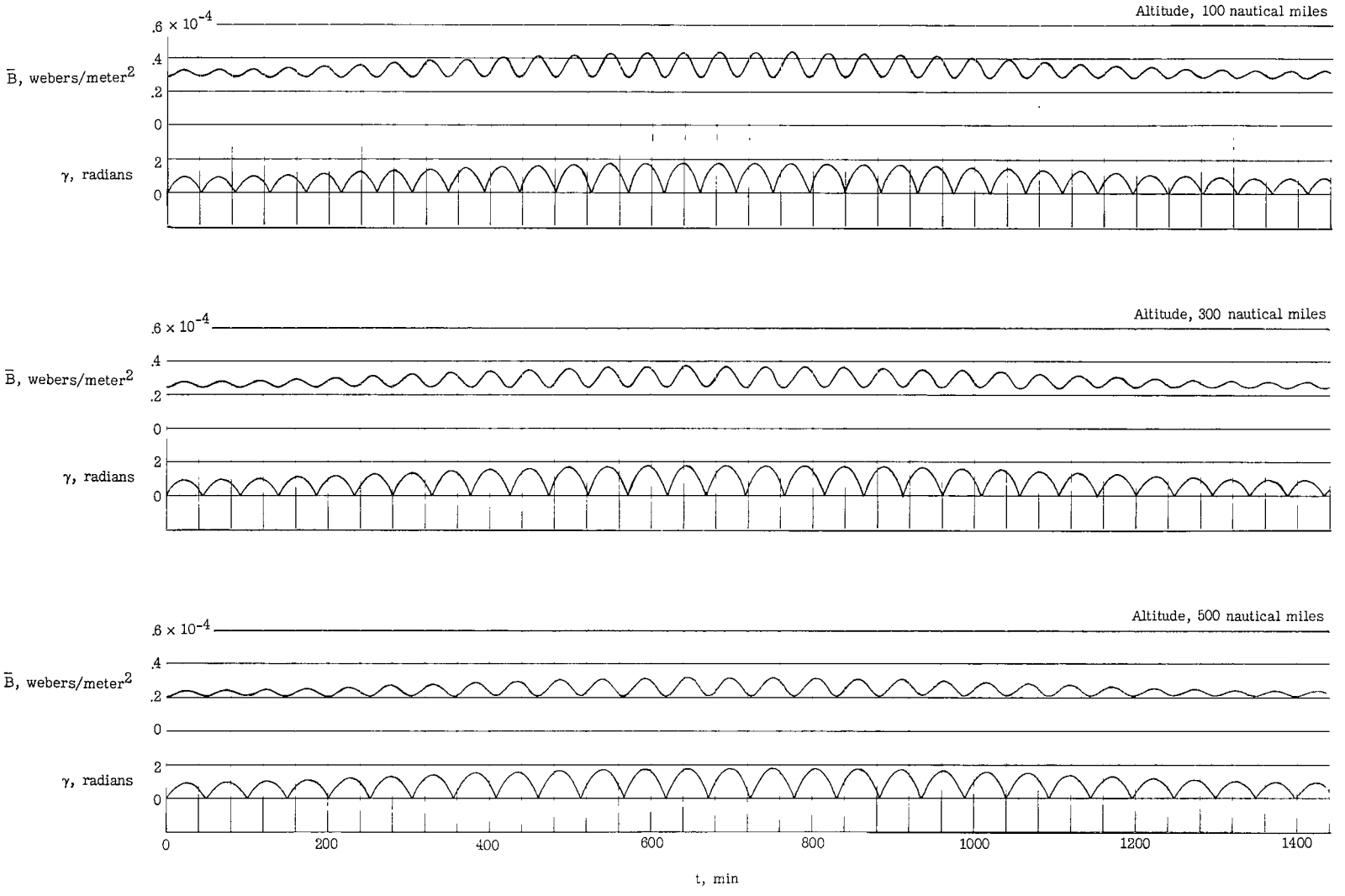

(c) $i = 30^{\circ}$.

Figure 4.- Continued.

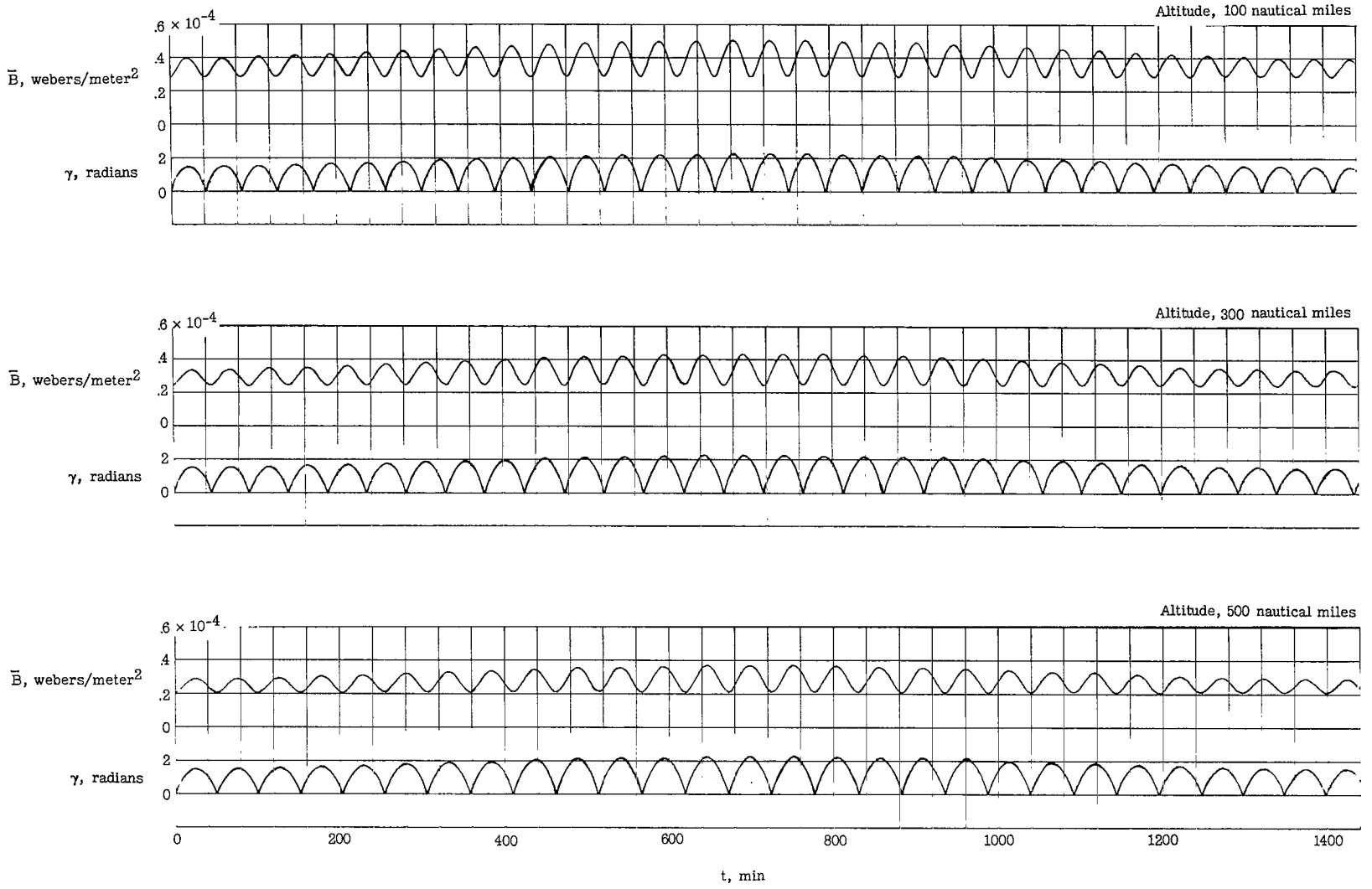

(d) $i = 45^\circ$.

Figure 4.- Continued.

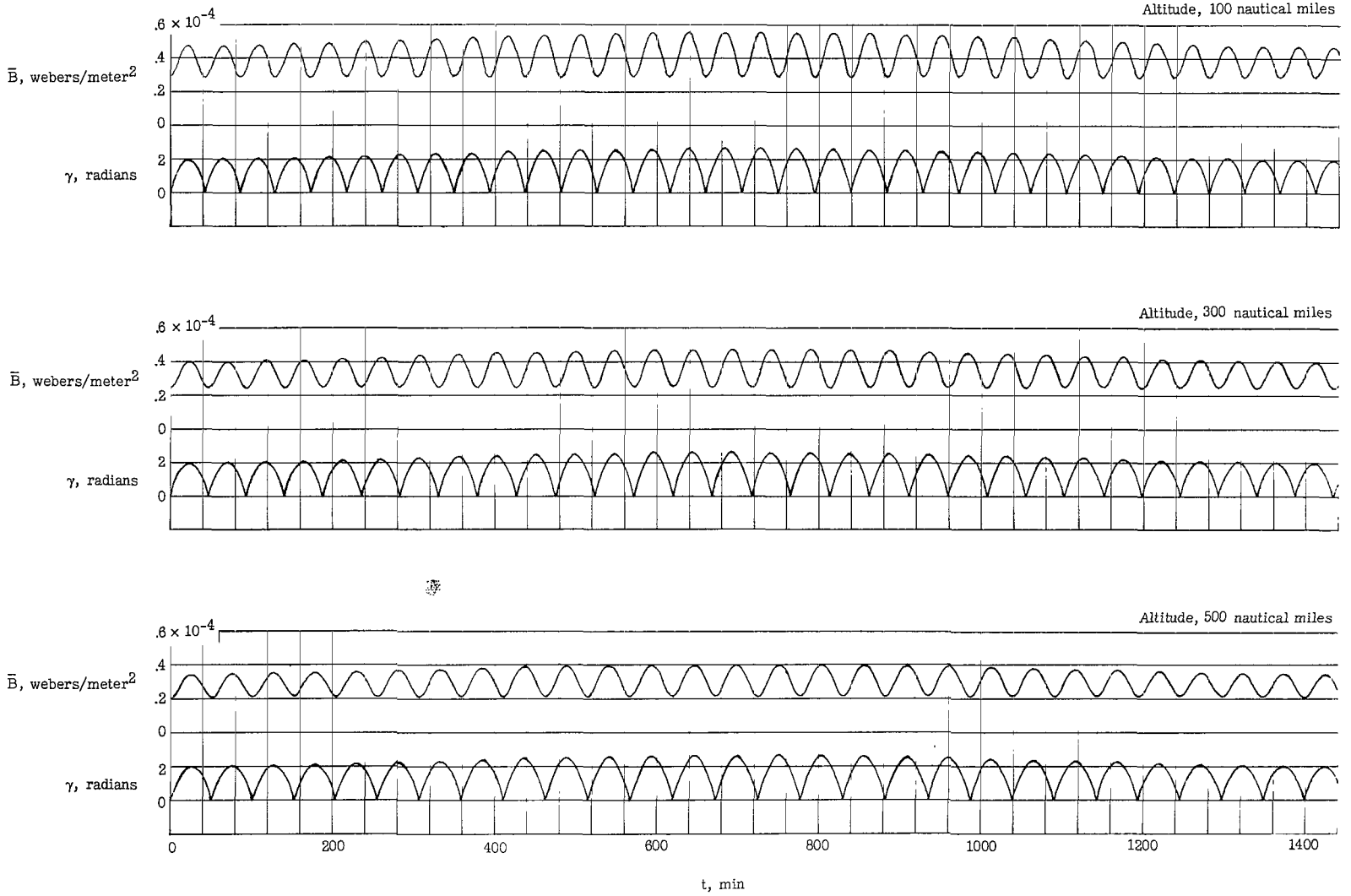

(e) $i = 60^{\circ}$.

Figure 4.- Continued.

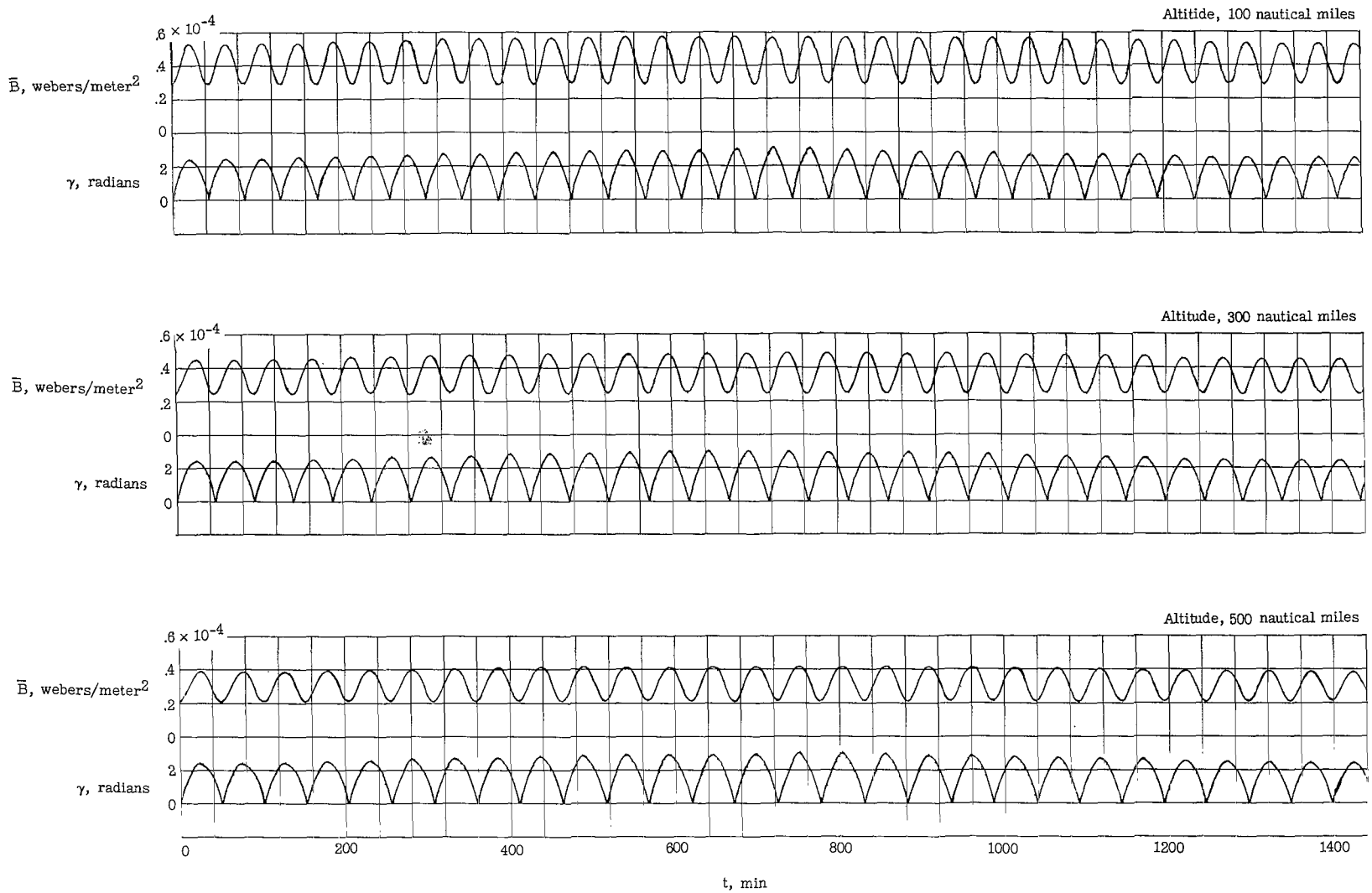

(f) i = 75°.

Figure 4.- Continued.

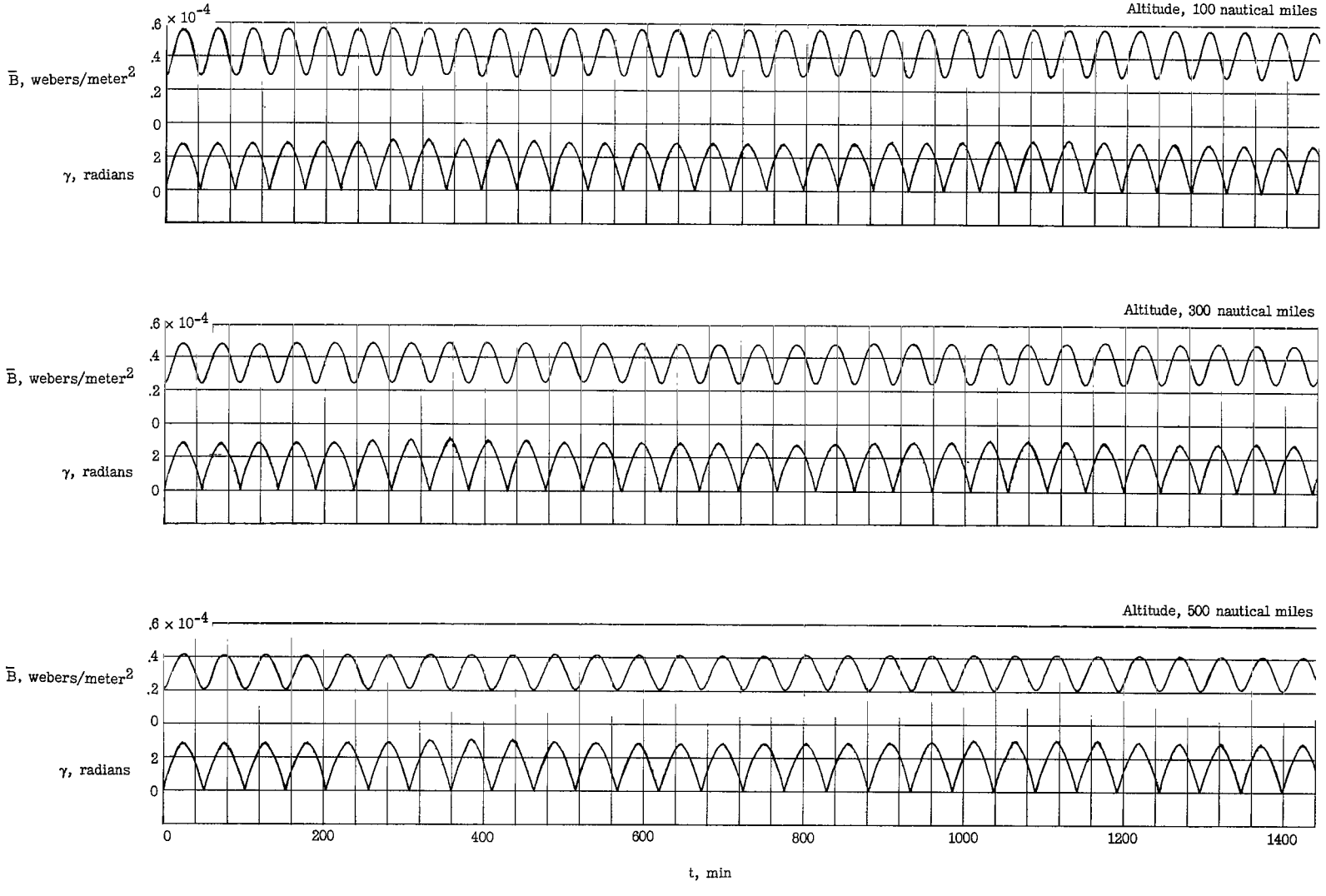

(g) i = 90°.

Figure 4.- Concluded.

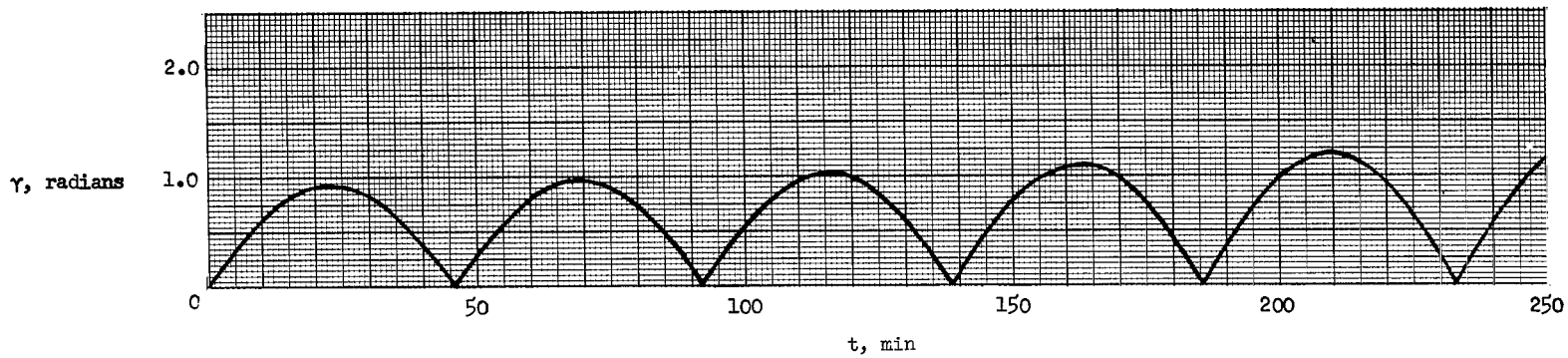

(a) $\phi_0 = 0.$

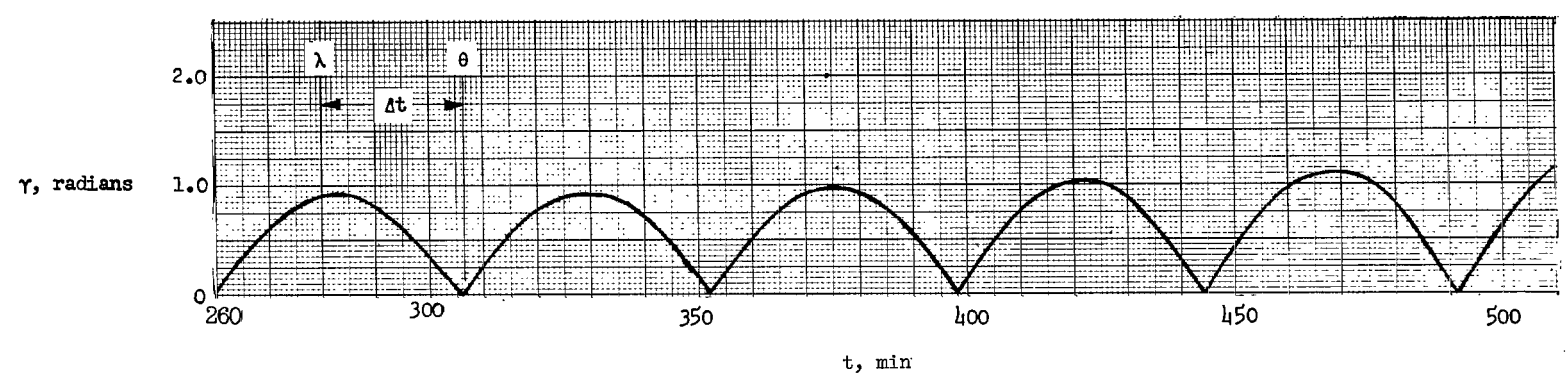

(b) ϕ_0 = 100 days.

Figure 5.- Comparison of time histories of γ for an orbital inclination of 30° at an altitude of 300 nautical miles.

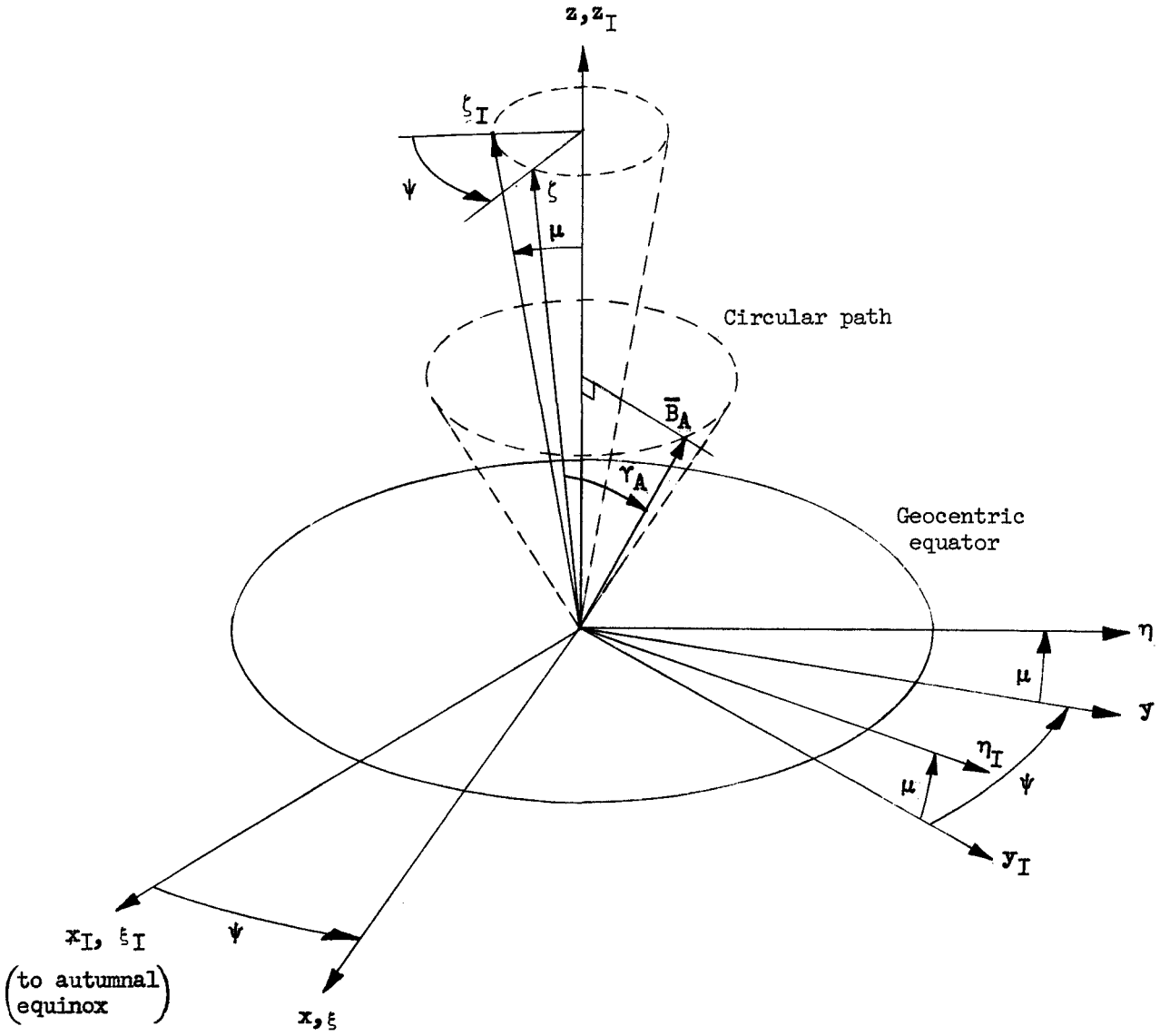

Figure 6.- Geomagnetic and geocentric inertial coordinate systems.

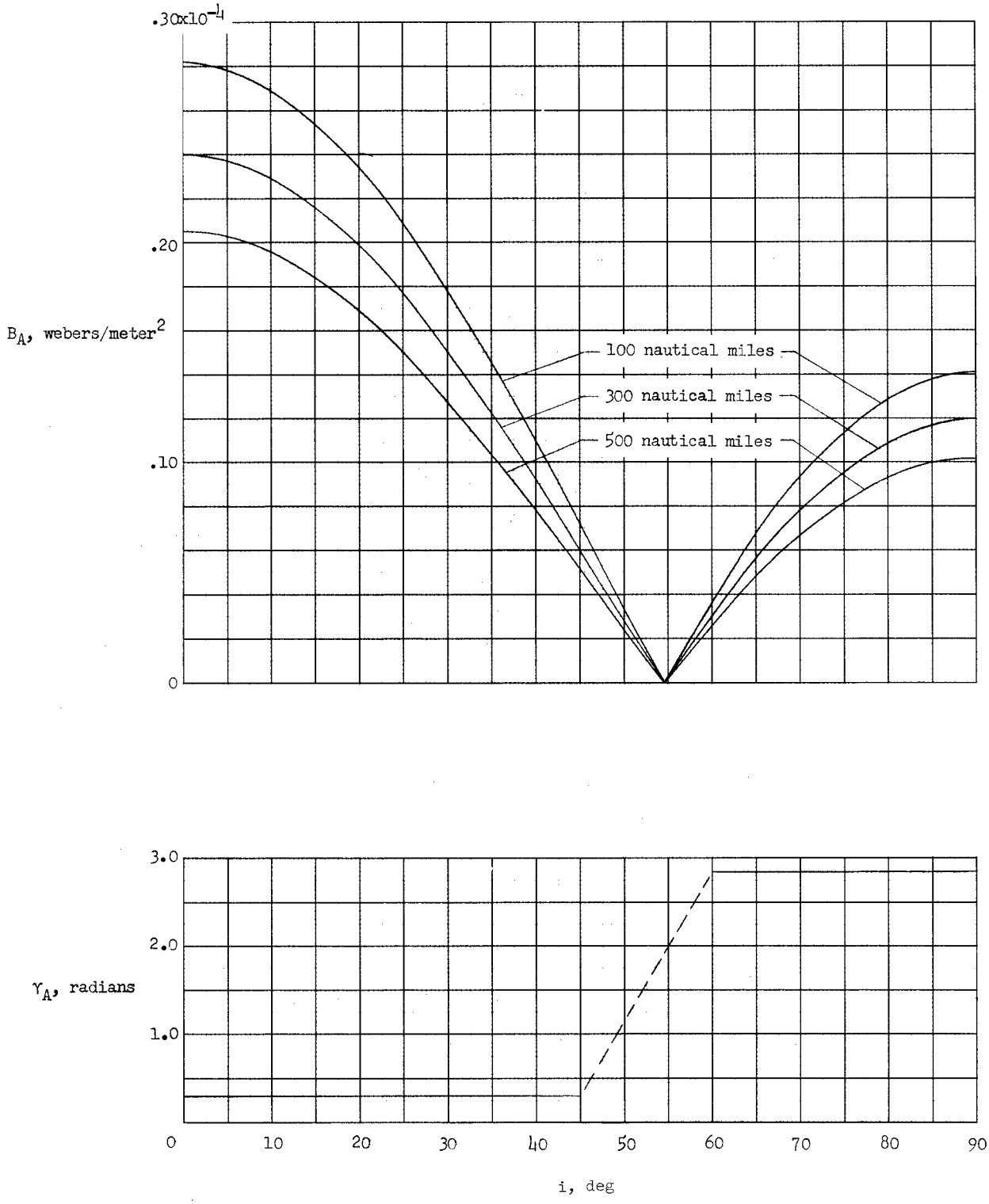

Figure 7.- Variation of average field intensity with orbital inclination in geomagnetic coordinates.

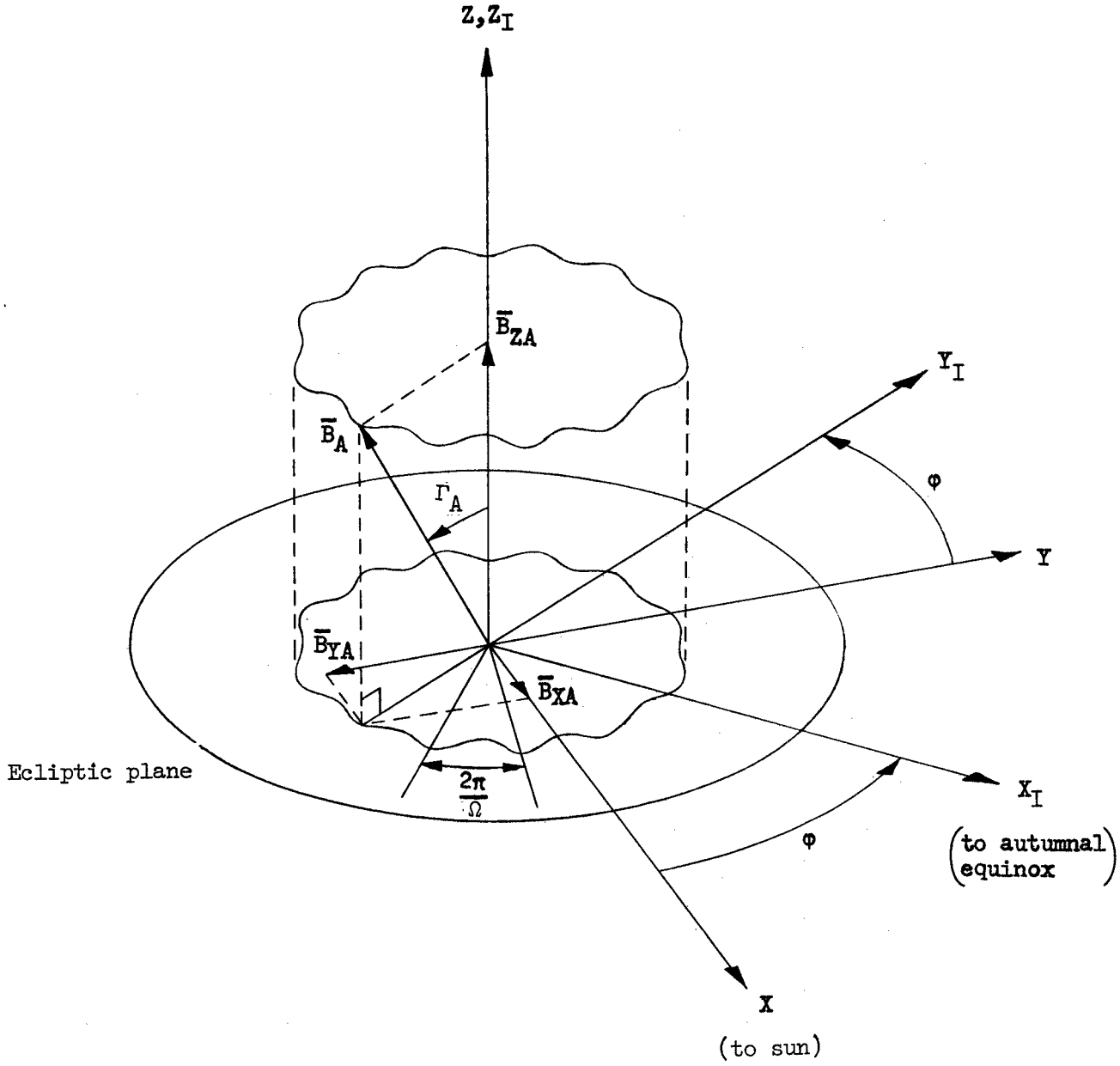

Figure 8.- Ecliptic inertial coordinate system.

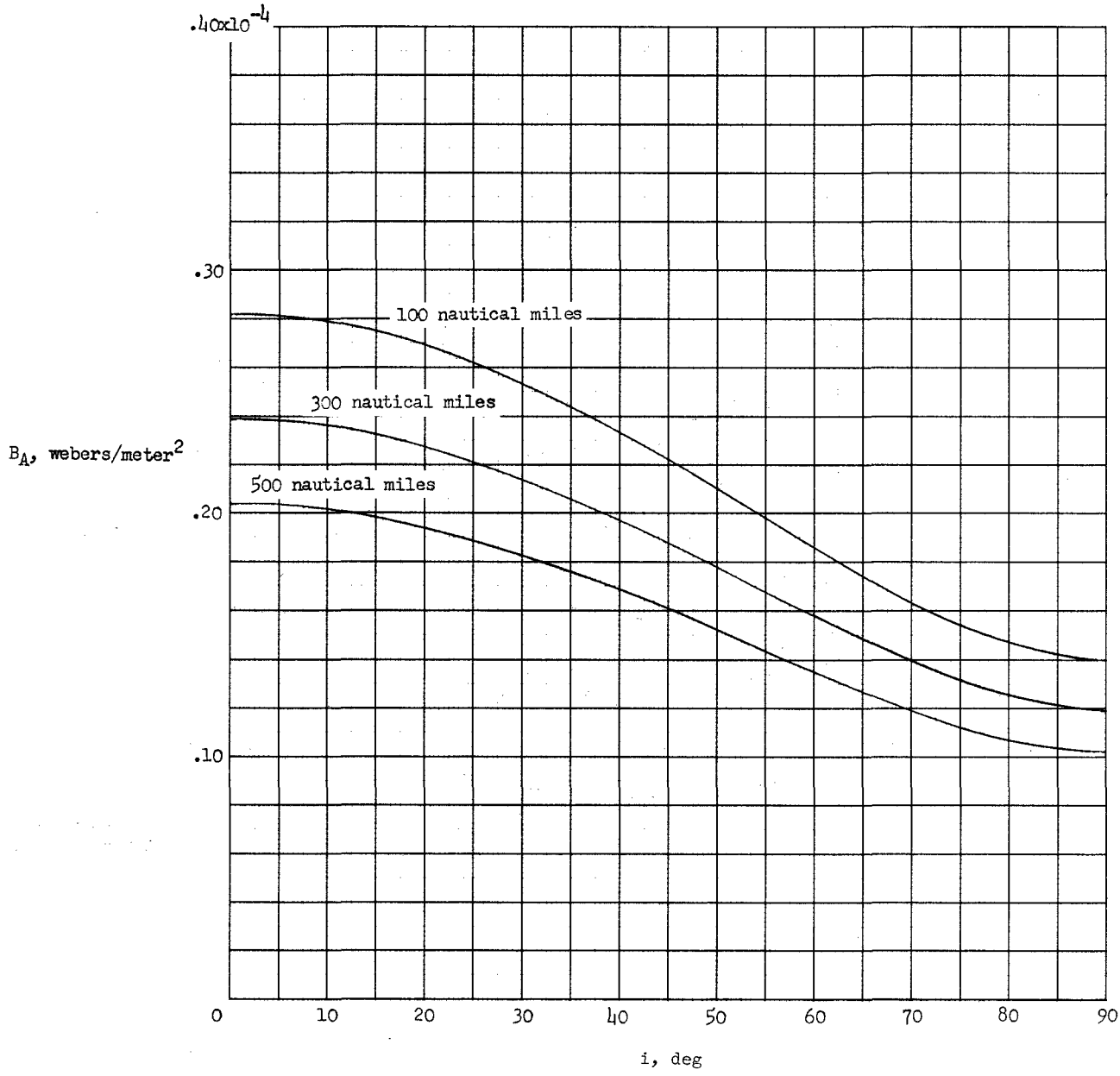

Figure 9.- Variation of average field intensity with orbital inclination in ecliptic coordinates.

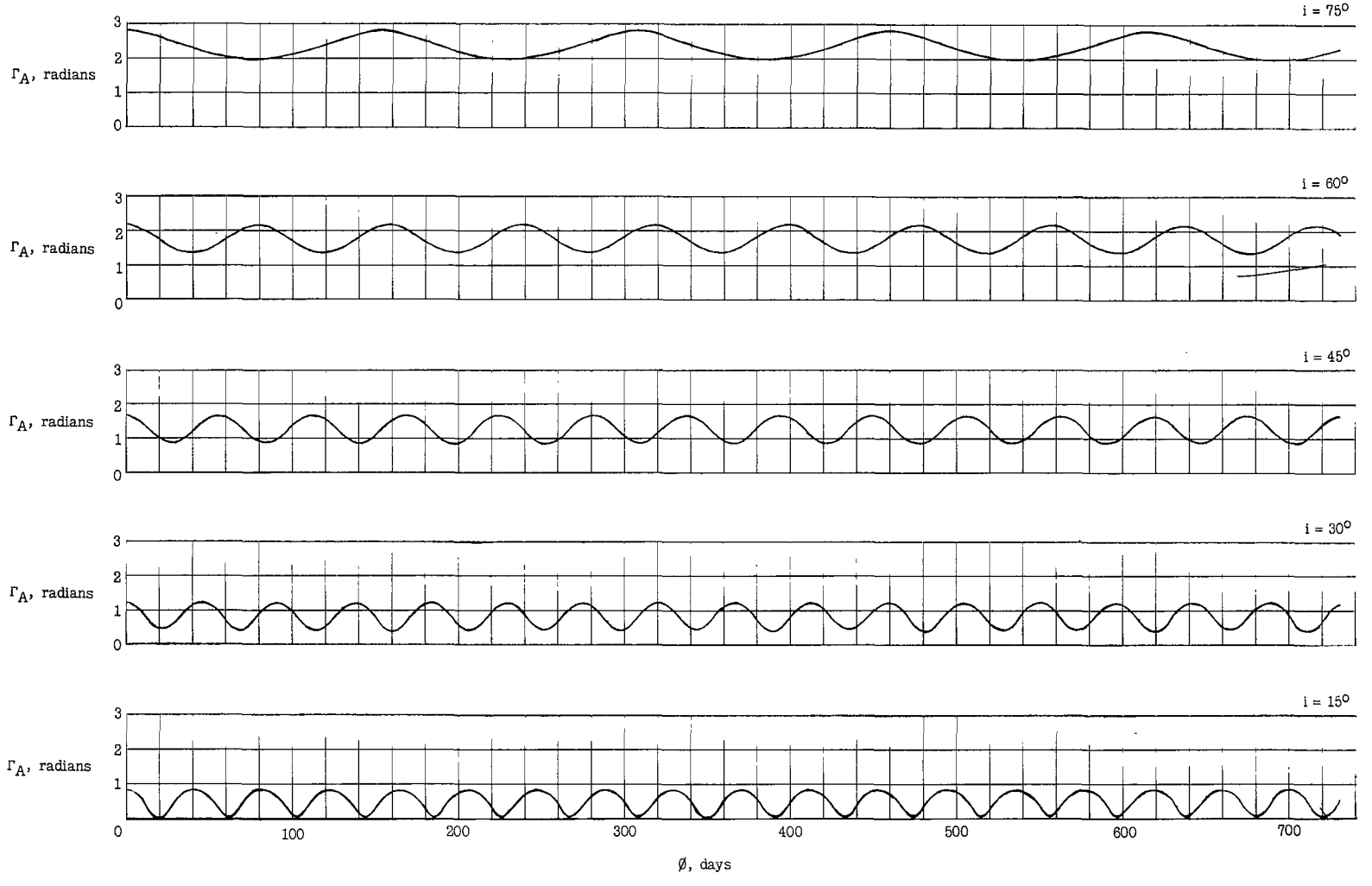

(a) Altitude, 100 nautical miles.

Figure 10.- Variation of the ecliptic average magnetic field with time.

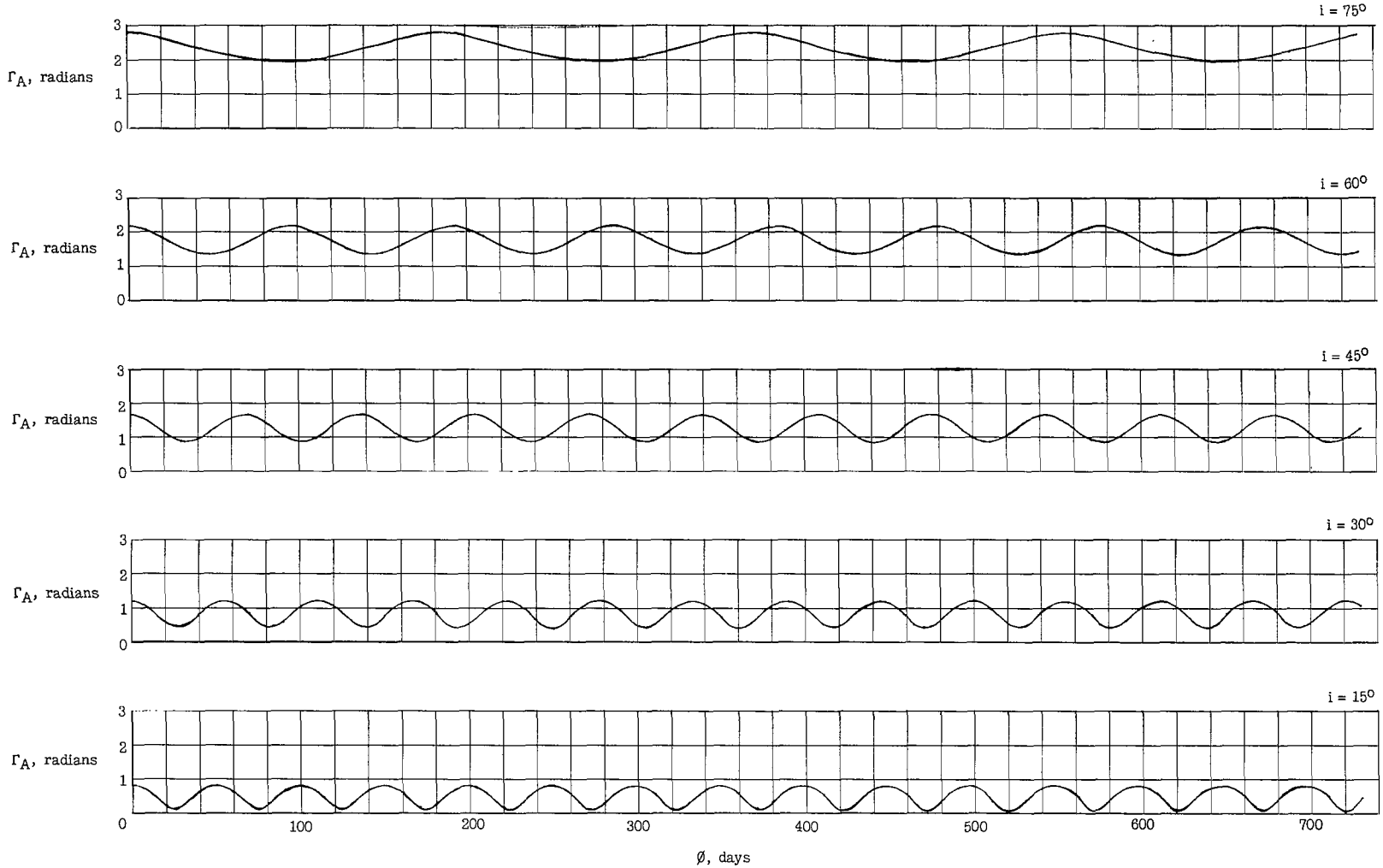

(b) Altitude, 300 nautical miles.

Figure 10.- Continued.

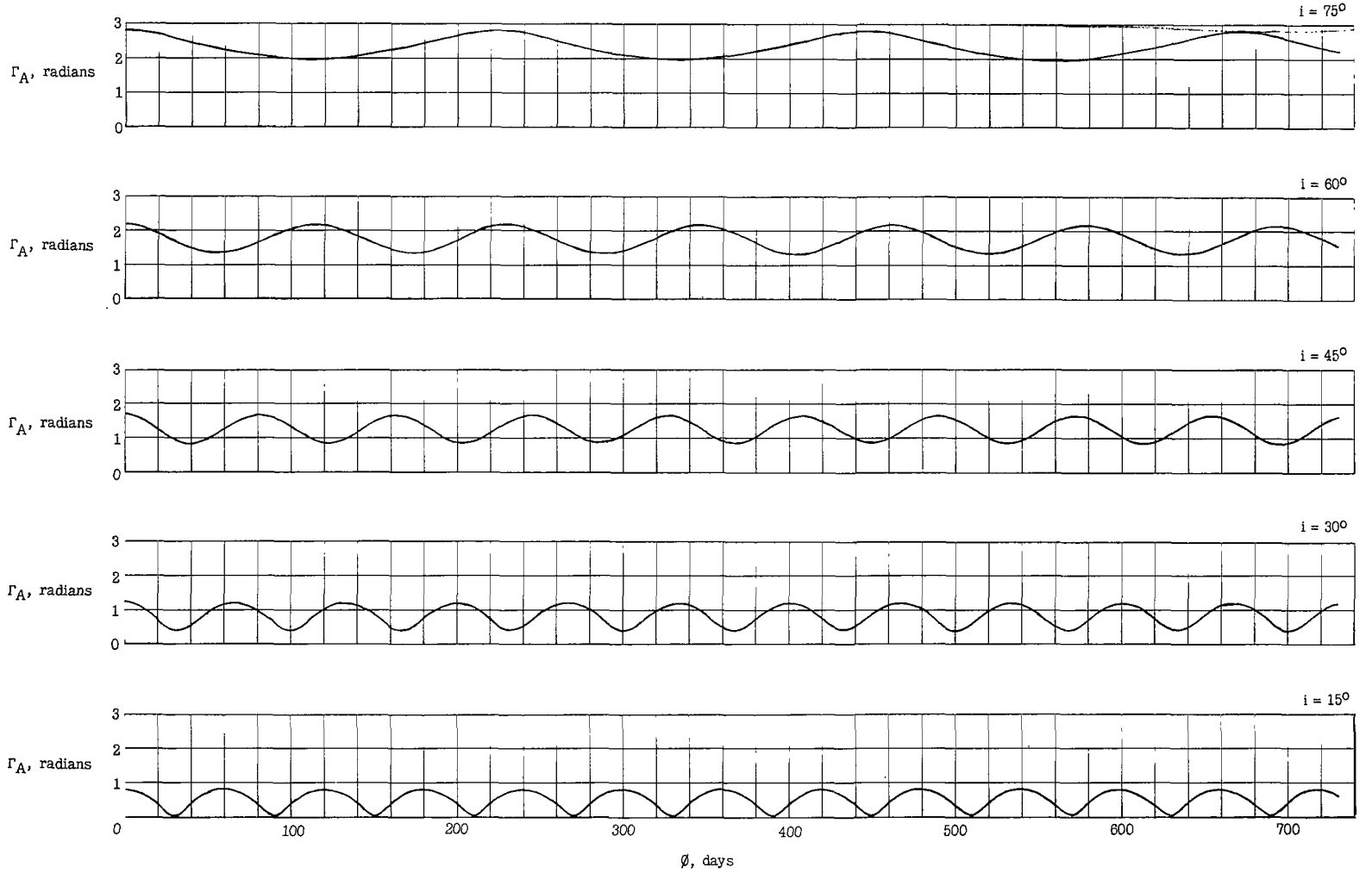

(c) Altitude, 500 nautical miles.

Figure 10.- Concluded.

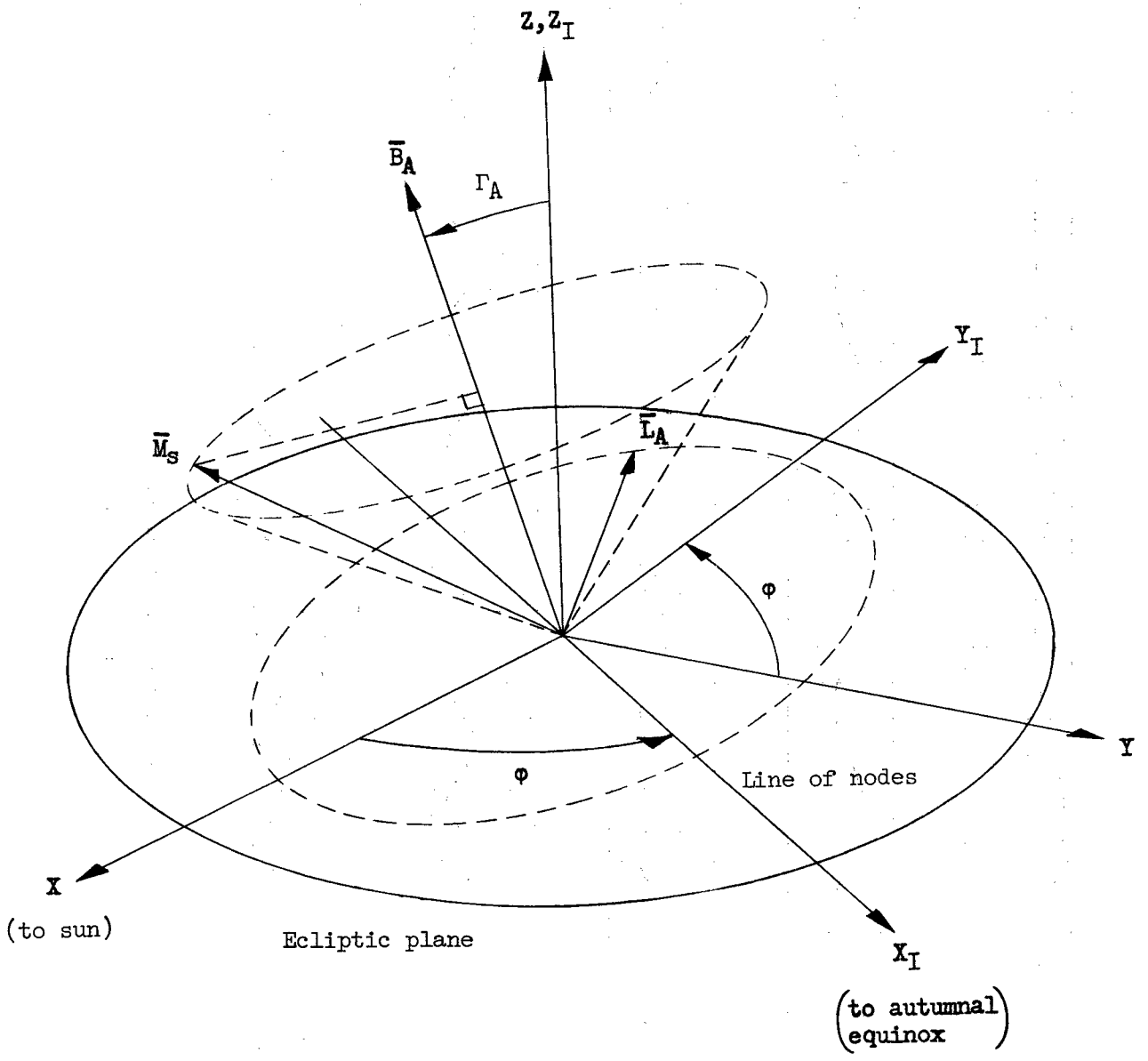

Figure 11.- Precession of satellite spin axis relative to the ecliptic plane.

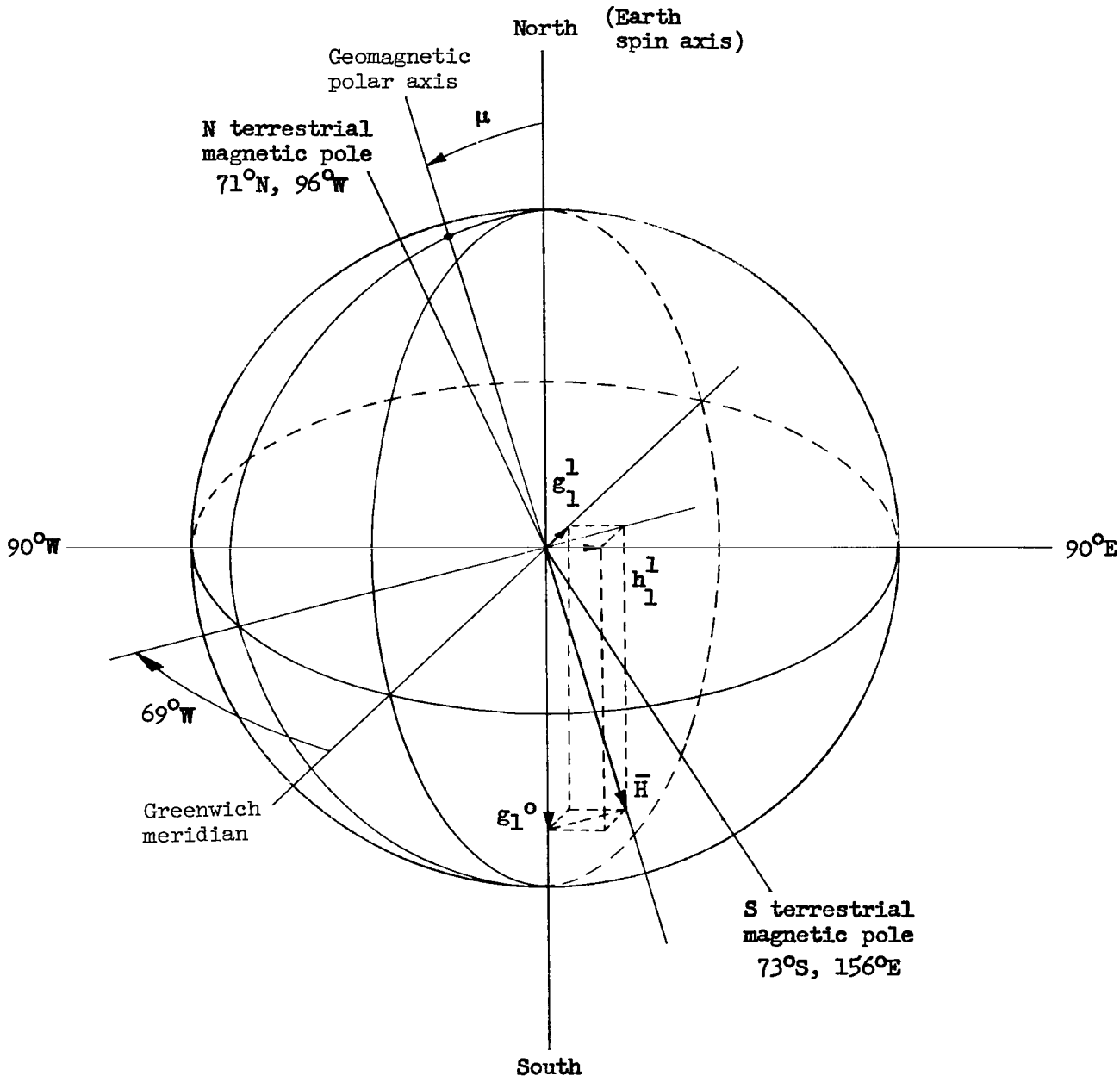

Figure 12.- Dipole representation of the earth's magnetic field.